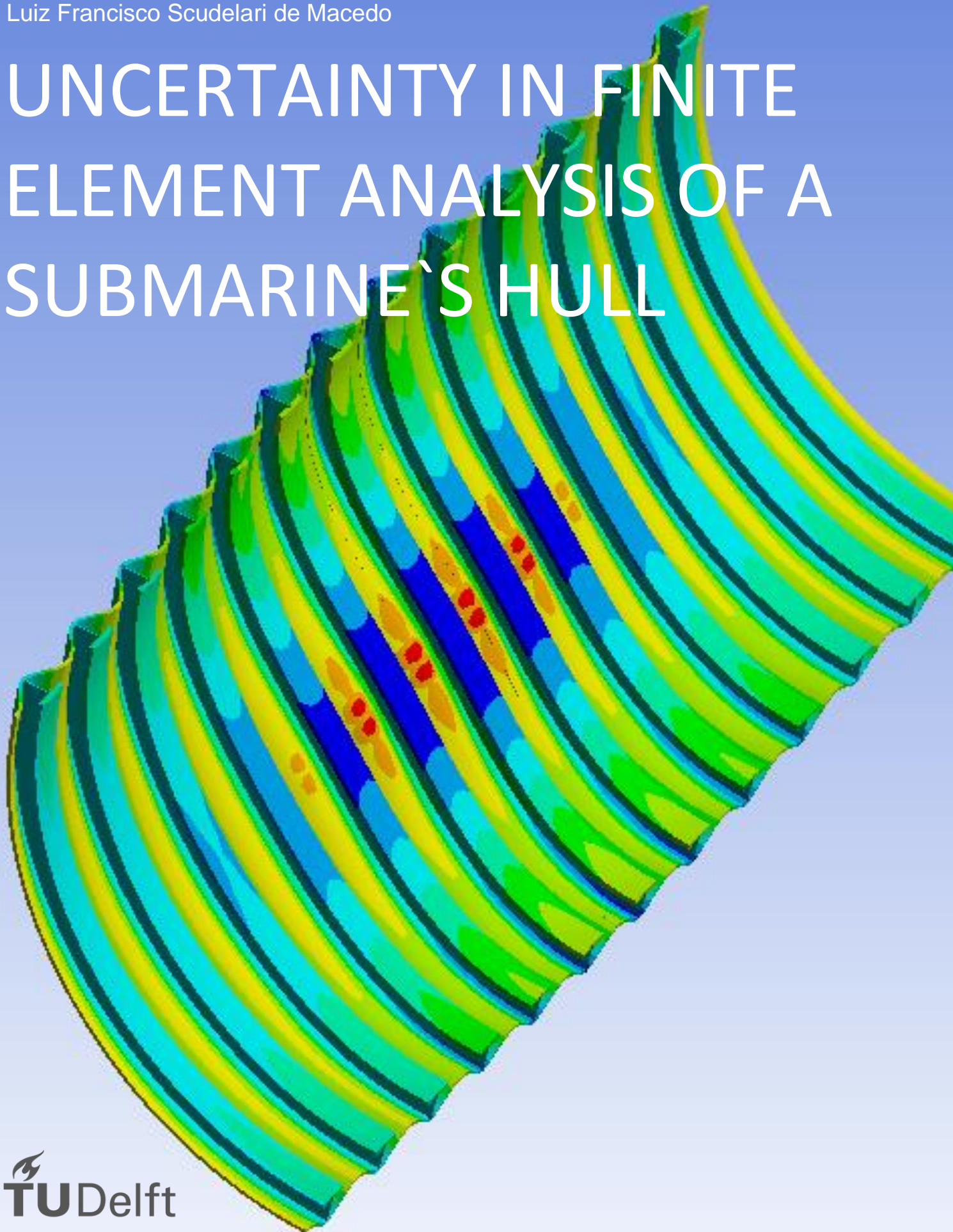


Luiz Francisco Scudelari de Macedo

UNCERTAINTY IN FINITE ELEMENT ANALYSIS OF A SUBMARINE'S HULL



UNCERTAINTY IN FINITE ELEMENT ANALYSIS OF A SUBMARINE`S HULL

By

Luiz Francisco Scudelari de Macedo

in partial fulfilment of the requirements for the degree of

Master of Science

in Offshore and Dredging Engineering

at the Delft University of Technology,
to be defended publicly on Tuesday January 16, 2020 at 08:30 AM.

| | | |
|-------------------|--------------------------|----------|
| Supervisor: | Ir. J. J. Reijmers, | TU Delft |
| Thesis committee: | Prof.dr.ir. M. Kaminski, | TU Delft |
| | Prof.ir. D. Stapersma, | TU Delft |
| | Dr. C.L. Walters, | TU Delft |

An electronic version of this thesis is available at <http://repository.tudelft.nl/>.

Preface

This research work investigates the deterministic uncertainty present in the results of Finite Element Models constructed to determine the collapse pressure of a typical submarine's hull. The study is performed as the thesis project required for the author's graduation as a Master of Science in Offshore and Dredging Engineering – Structural Analysis Track – at the TUDelft. This study was performed under the supervision of J.J. Reijmers and under general coordination of Prof. M. Kaminski. The subject for this research was determined as a possible assistance for the supervisor's Phd work related to the probabilistic design of submarine's pressure hull, this work being developed also for the TUDelft. The results obtained show that small uncertainty is present in models prepared by Expert Performers, but larger scatter might exist when models are constructed by Advanced Beginners. Also, other insights related to contrasting FE results to the expected behaviour from traditional analytical analysis are presented throughout the document.

*L.F. Scudelari de Macedo
Delft, January 2020*

Contents

| | | |
|----------|--|-----------|
| 1 | Introduction | 11 |
| 2 | Problem Statement | 13 |
| 3 | Theoretical Background and Literature Review | 15 |
| 3.1. | The Finite Element Method | 15 |
| 3.2. | Types of Errors in Finite Element Method | 17 |
| 3.3. | Meshing and Mesh Size | 18 |
| 3.4. | Shell Element Types and Order | 19 |
| 3.5. | Element's In Plane Integration Scheme | 20 |
| 3.6. | Position and Number of Integration Points Through the Thickness | 20 |
| 3.7. | Geometrical Nonlinearities and Large Deflections | 21 |
| 3.8. | User's Level of Expertise | 21 |
| 3.9. | Similar Studies from Other Authors | 22 |
| 4 | Methodological Approach | 23 |
| 4.1. | Reference Geometry | 23 |
| 4.1.1. | The Manatee Class | 23 |
| 4.1.2. | Detailed Geometry Modelled and Out-of-Circularity | 24 |
| 4.2. | Axis Convention and Coordinate System | 25 |
| 4.3. | General Modelling Parameters | 25 |
| 4.3.1. | Material | 25 |
| 4.3.2. | Loading | 26 |
| 4.3.3. | Boundary Conditions | 27 |
| 4.3.4. | Linear Elements Near the Bulkheads | 28 |
| 4.3.5. | Meshing | 29 |
| 4.4. | Identification of the Constructed Models | 30 |
| 4.5. | Arrangement of The Parameters for Each Level of Expertise | 31 |
| 4.6. | Verification of Models | 33 |
| 4.7. | Responses of Interest and Failure Criteria | 35 |
| 4.8. | Statistics and Uncertainty Quantification | 37 |
| 5 | Analysis and Discussion of the Results | 38 |
| 5.1. | Software | 38 |
| 5.2. | Non-linear Settings | 38 |
| 5.3. | Model Quantities and Run Time | 39 |
| 5.4. | Mesh Convergence Studies | 39 |
| 5.5. | Results and Their Uncertainty Quantification | 40 |
| 5.5.1. | Uncertainty Quantification Within Each Level of Expertise Group | 40 |
| 5.5.2. | Uncertainty Quantification Between Different Levels of Expertise | 49 |
| 6 | Conclusions | 51 |

Abstract

The Finite Element Method possess the intrinsic characteristic that, due to the assumptions made for the parameters of the problem being modelled, a deterministic uncertainty on the obtained results is always present. This research makes use of basic statistical concepts to obtain reference values for a possible quantification of this uncertainty. The problem used as basis for the analysis is the determination of the hydrostatic pressure which leads to the failure of the central compartment of a Manatee class submarine, by means of non-linear analysis with imperfections included. To generate a set of possible result outcomes, key parameters used in the construction of a model are varied in order to ensure the production of both model-form and solution approximation errors. The parameters varied are four, namely (1) the in-plane integration scheme, (2) the order of the shell elements (3) the small displacements assumption and (4) the mesh size. The produced variation is then grouped in sets related to three different possible analyst's levels of expertise and the uncertainty is quantified for the data both within and in between groups. The analysis show that only a small uncertainty can be expected in the results from non-linear models constructed by Expert Performers (with the 95th quantile being up to 3.94% larger than the estimated average), but larger scatter is present if outcomes from Advanced Beginners are considered (the maximum 95th quantile in non-linear results is 10.30% larger than the estimated average). If no information is provided on the expertise level of the analyst who produced a model, from comparing the results in between sets, an uncertainty of up to around 12% might be expected for the pressure which induces yield. Other results of interest are described throughout the document, like a post flange yield result which can put current analytical assumptions of global collapse into a different perspective and the impact that varying the parameters have on the first yield location.

Acknowledgements

The author is grateful to Jack Reijmers for the valuable debates, to Prof. Kaminsky for the pragmatism, to his Brother and Wife for the patience and to his Parents for the example to follow.

List of Symbols

| | |
|-----------------------------|---|
| 95_quantile | Ninety fifth Quantile |
| B | matrix which relates strains and displacements |
| bf | Flange width |
| CSR | Common Structural Rules |
| DNV-GL | Company which is an International accredited registrar and classification society |
| <i>E</i> | Young's modulus |
| <i>F</i> | Resultant forces within a domain |
| FE | Finite Element |
| FEM | Finite Element Method |
| hw | Web depth |
| IACS | International Association of Classification Societies |
| ISSC | International Ship and Offshore Structures Congress |
| k | element's stiffness matrix |
| K | Stiffness matrix |
| $\overset{t}{k}$ | tangent stiffness matrix at time step i |
| $\overset{t}{K}$ | tangent stiffness matrix |
| $\overset{l}{s}K$ | linear stress stiffening matrix generated from obtained perturbation stresses |
| Lf | Frame spacing |
| NLFEM | Non Linear Finite Element Method |
| P_{1st_yield} | Hydrostatic pressure which would lead to the first yield of any structural component of the model |
| $P_{center_yield_midbay}$ | Hydrostatic pressure which would lead to the yielding of the hull's plate center at the interframe midbay |
| P_{flange_yield} | Hydrostatic pressure which would lead to the yielding of the outer fiber of a ring stiffener flange |
| P_{last_conv} | Hydrostatic pressure which is obtained at the last converged analysis step |
| $P_{lin_buckling}$ | Hydrostatic pressure related to the Linear Buckling Eigenvalue of the first mode |
| R | Inner radius of the pressure hull |
| R | nodal forces |
| $\overset{t+\Delta t}{R}$ | vector which lists the externally applied nodal point forces in the configuration at time $t + \Delta t$ |
| Rm | Mean radius of the pressure hull |
| R_{perturb} | Applied perturbation external loads for linear buckling analysis |
| s | Thickness of the pressure hull |
| sf | Flange thickness |
| SHELL181 | Linear Shell Element in Ansys named SHELL181 |
| SHELL281 | Quadratic Shell Element in Ansys named SHELL281 |
| ST_DEV | Standard Deviation |
| sw | Web thickness |
| <i>u</i> | field displacements in <i>x</i> |
| U | displacement's degrees of freedom |
| <i>U₉₅</i> | Quantified Uncertainty by the 95th Quantile |
| <i>U_{CV}</i> | Quantified Uncertainty by the Coefficient of Variation |
| U_{perturb} | Set of perturbation displacements related to R_{perturb} in linear buckling analysis |
| ULS | Ultimate Limit State |
| V | 3-D domain |
| <i>v</i> | field displacements in <i>y</i> |

GREEK LETTERS

| | |
|--------------------------------|--|
| γ_{xy} | Shear Strain |
| $\epsilon_{xx}, \epsilon_{yy}$ | Normal Strains |
| λ_i | Buckling eigenvalues |
| ν | Poisson's ratio |
| τ | Time step at the eminence of buckling collapse |
| τ_{xx}, τ_{yy} | Normal Stresses |
| τ_{xy}, τ_{yx} | Shear Stresses |
| Φ_i | Buckling eigenvectors |

List of Tables

| | |
|---|----|
| Table 1 - Model Types | 30 |
| Table 2 – Mesh Classification | 31 |
| Table 3 – Model parameters for each Level of Expertise | 33 |
| Table 4 – Location of first yield per model type and mesh size | 35 |
| Table 5 – Student’s t-distribution one-sided quantiles of interest..... | 38 |
| Table 6 – Model Quantities | 39 |
| Table 7 - Expected Uncertainty in Results obtained by Advanced Beginners Analysts | 41 |
| Table 8 - Expected Uncertainty in Results obtained by Competent Performers Analysts | 44 |
| Table 9 - Expected Uncertainty in Results obtained by Expert Performers Analysts | 47 |
| Table 10 - Ratio 95th quantile [adv_begginer] / Average [expert performer] | 50 |

List of Figures

| | |
|---|----|
| Figure 1 - Overview of the Manatee class pressure hull | 23 |
| Figure 2 - Dimensions of the Manatee Class Pressure Hull | 24 |
| Figure 3 – Overview of the FE model..... | 24 |
| Figure 4 – Imperfect shape (amplified 20x)..... | 25 |
| Figure 5 – Coordinate System..... | 25 |
| Figure 6 – HY80 material curve considered..... | 26 |
| Figure 7 – Application of external hydrostatic pressure of 10Mpa | 26 |
| Figure 8 – Longitudinal force of 71.3kN | 27 |
| Figure 9 – Symmetry over z axis (affected edges in red) | 27 |
| Figure 10 – Symmetry over y axis (affected edges in red) | 28 |
| Figure 11 – Rigid support both for translations and rotations (affected edges in yellow) | 28 |
| Figure 12 – Rigid support at load application edge (only translation in “x” is allowed). All nodes at the edge are coupled for translation in “x” | 28 |
| Figure 13 - Regions at the hull with elastic material (in darker grey) | 29 |
| Figure 14 - Very fine mesh (20 elements interframe)..... | 29 |
| Figure 15 - Very coarse mesh (3 elements interframe) | 30 |
| Figure 16 - Maximum displacement when a typical model reaches yield at midbay | 32 |
| Figure 17 - Comparison for verification. Left - Results by the author; Right - Results by the thesis supervisor..... | 34 |
| Figure 18 – Mesh Convergence study for the Eigenvalue Buckling Pressure – Log Scale..... | 39 |
| Figure 19 - Mesh Convergence study for the pressure which induces yielding of the hull’s plate center at the interframe midbay– Log Scale | 40 |
| Figure 20 - Possible Results by Advanced Beginners - <i>Pcenter_yield_midbay</i> | 41 |
| Figure 21 - Possible Results by Advanced Beginners - <i>Plast_conv</i> | 42 |
| Figure 22 - Possible Results by Advanced Beginners - <i>P1st_yield</i> | 42 |
| Figure 23 - Possible Results by Advanced Beginners - <i>Plin_buckling</i> | 43 |
| Figure 24 - Possible Results by Advanced Beginners - <i>Pflange_yield</i> | 43 |
| Figure 25 - Possible Results by Competent Performers - <i>Pcenter_yield_midbay</i> | 44 |
| Figure 26 - Possible Results by Competent Performers - <i>Plast_conv</i> | 45 |
| Figure 27 - Possible Results by Competent Performers - <i>P1st_yield</i> | 45 |
| Figure 28 - Possible Results by Competent Performers - <i>Plin_buckling</i> | 46 |
| Figure 29 - Possible Results by Competent Performers - <i>Pflange_yield</i> | 46 |
| Figure 30 - Possible Results by Expert Performers - <i>Pcenter_yield_midbay</i> | 47 |
| Figure 31 - Possible Results by Expert Performers - <i>Plast_conv</i> | 48 |
| Figure 32 - Possible Results by Expert Performers - <i>P1st_yield</i> | 48 |
| Figure 33 - Possible Results by Expert Performers - <i>Plin_buckling</i> | 49 |
| Figure 34 - Possible Results by Expert Performers - <i>Pflange_yield</i> | 49 |
| Figure 35 - Uncertainty Comparison between different levels of expertise for <i>Pflange_yield</i> | 50 |

1 Introduction

“Models are to be used, not believed.”

H. Theil

The concept behind the quote above is what brings the impetus for the present research. In engineering practice, models are constructed to allow for the prediction of capacities and behaviours related to how the design object will respond to the future demands it will be subjected to. Modelling is an activity somehow related to fortune-telling or the ancient practice of palm-reading where information in the present time and input parameters are threaded and analysed and, from this process, future possible outcomes are accessed.

Obviously in the engineering context the created models have a much more robust scientific background than the models constructed from instinct and experience which govern palm-reading, but even scientifically accepted models need to count on assumptions and simplifications in order to be workable with. So, in the same manner that advices from fortune tellers must be taken with caution, care should be taken when making use of results obtained from mathematical models. When one captures an intended response to be used for design, it is important that the obtained value is understood as just one materialization of a range of possible outcomes, and a variation between the value from the model and the real-life value is unavoidable.

Also, models are constructed by people, with different experiences, intentions and background. The same physical problem will most probably be modelled differently by different analysts, with the level of expertise being a determinant factor on the correctness of the outcomes.

This work aims then in contributing on the understanding of how much deterministic variability may exist in model results used to derive the capacity that a typical submarine's compartment possesses to withstand water pressure while submerging. More specifically, the results obtained from Finite Element Method models performed using practices and under assumptions which are in general accepted by the engineering practitioners' community and included in recognized design procedures, but which are performed by analysts with different levels of expertise.

The geometry for the structural problem in the background of this research is the stiffened cylindrical shell of a typical submarine. In the studied case, the selected class is a Manatee Submarine. Only one geometry is analysed with only one set of geometrical and environmental parameters, i.e. for the entire research the same boundary conditions, materials, loading, imperfections, etc. are used. This is made in order to keep the focus of the research on the possible variability which comes from the modelling parameters which are often under the analyst's choice, and not inputs for a given problem.

The subject might be of interest to Maritime engineers; Naval architects or Structural engineers in general. Any professional who makes use of results from Finite Element modelling in decision making for the design of structures which somehow relate to the geometric typology of the cylindrical stiffened shell used as basis for this research, might be interested in this subject. By appreciating the results, the reader will gain a better intuition on how to apply proper load factors during design or on how much the results from finite element analysis might be varying from perfect analytical solutions. It is expected that the reader is familiar with structural mechanics and the Finite Element Method (even in just a superficial manner which allows for its day-by-day application in simple problems) and also has basic knowledge on statistics.

The research is performed by exploring solely deterministic uncertainties in finite element modelling (i.e., the stochastic nature of modelling inputs is not included in this research). The uncertainty exploration is performed by means of understanding what are the impacts in characteristics responses which arise from the variation of typical Non-Linear Finite Element Method (NLFEM) parameters. A vast range of possible

parameters to be changed exist, and a selection of the most representative ones had to be made to keep the focus for this research.

From the geometrical characteristics of the plated structures analysed, shell elements are the best applicable. In this work it is assumed that the parameters which usually yields to the higher doubts from the analyst on its application are: The order of the elements to be used; The integration scheme; The validity of the small displacements assumption; and, naturally, the meshing. By varying those four parameters for a same problem, several responses are captured, grouped into possible outcomes from defined levels of expertise, and their uncertainty measured by means of basic statistical treatment of the data.

The setting of parameters of an analysis is a process which rely on the experience and intuition of the analyst using the finite element framework. In the proceedings of the 19th International Ship and Offshore Structures Congress (ISSC) [1], the committee who performed benchmark studies concluded that:

“... the successful use of NLFEM still relies on analysts having a high degree of expertise in constructing the finite element model, sound engineering judgement to evaluate the uncertainty of the results and knowledge regarding the limitations for a given finite element program”

So, the research can also be seen as dealing with this user related aspect, in the sense that different analysts may decide to select different ways to solve the same problem.

For sure model parameters which are wrong must be excluded from the analysis made by Expert Performers. So, the models which were generated as related to this level of expertise attempted to be as close as possible to the recommendations for finite element modelling from a company which is an International accredited registrar and classification society named DNV-GL [2].

All the analysis in this research were performed using the Ansys 2019 R01 Mechanical software package. The Workbench environment is used as the form for the data input.

This document is organized attempting to be as close as possible to the traditional scientific methodology for information presenting. First the existing problem which generates the investigation is described in the Problem Statement chapter. Nuances of the research motivation and some specific aspects of the problematic are outlined, and the research question is clearly defined. Then the current status of knowledge on the subject and important aspects of each parameter explored are presented in a generalist manner in the Theoretical Background and Literature Review section. Important technical concepts related to the methodology used are presented in a manner that the reader would be at least familiar with the ideas debated or guided to the bibliographic references where such knowledge can be better explained. The information which allows for the recreation of the analysis performed are present on the chapter Methodological Approach. It also contains description on the procedures used for the verification of the models and other important information with respect to the captured responses. The results obtained are presented at the chapter Analysis and Discussion of the Results. In this chapter the statistical quantities which would allow the use of this research in other problems are also derived and presented. Finally, the Conclusion chapter interprets the results and proposes several manners in which this research can be further extended.

2 Problem Statement

The Finite Element method is a modelling strategy which allows for the solution of the set of differential equations which govern the mechanical behaviour of structures. By making use of the weak form of such equations, it allows for the treatment of the problem related to a continuum domain by the use of an approximated equivalent discrete domain, where the set of equations gain a simpler format which can be then solved numerically. Of course, there is a trade-off related to the precision of the results and a solution approximation deterministic error is always present.

Assumptions for the parameters used in the transformation from a continuous domain to a discrete domain are then made related to the physics and mathematics of the problem, aiming in increasing the precision and decreasing the computational effort. Such assumptions involve for example the order of the required interpolation functions and the numerical scheme for the necessary integrations involved in the finite element method.

It is intuitive to grasp that a major aspect of such strategy is how the discretization of the problem (the meshing) is set. Obviously with very small discrete elements with relation to the problem's scale, the closer the model is to an actual continuum problem, and the errors tend to be smaller. One might expect that an infinitely dense mesh would lead to the same results as the continuum problem with disregard of assumptions like the order of interpolation functions (in practice this is limited to the case when small numerical errors sum up). But in the other hand, the smaller the elements, the larger the quantity of degrees of freedom for the analysis and the larger the numerical computational effort in order to solve the equations. Also, there are cases in which some dimensions of the problem do not allow for proper discretization due to different magnitudes in the geometric scale depending on the direction. An example of this is the discretization in the through thickness direction of shells. In this case the physics assumptions in that direction for the elements is kept independently on the selected mesh size.

In the end the solution of a problem related to a continuum by means of its discretization always require a compromise. Frey [3] states that:

“... an optimal mesh is that for which the chosen quality function is optimal while, at the same time, its number of vertices (elements) is minimal. In practical terms, it may be concluded that the optimal mesh is that which gives a suitable compromise between various criteria.”

Such compromise in current industrial practice is not only problem dependent but also related to human judgement. Even for advanced analysis when a proper meshing quality function is mathematically defined, its specification is determined by the user and several criterions are available for such a function [3]. Evidences of the user dependency aspect can be seen on the results obtained in Finite Element Method benchmark studies of plated structures performed for the ISSC 2015 and 2018 congresses [1] [4], when different participants got different responses for a given problem with direct differences of up to 70% in their captured response values.

In practice, for real-life simulation problems, timing and resources play a major role on how finite element analysis are performed. It is often the case that the resulting model-form and solution approximation errors in the analysis will be impacted by schedule availability and the experience of the analysts in setting the parameters which, under his judgement, will lead to a suitable compromise between numerical efforts and precision.

Rules and literature exist on the practical aspects to perform finite element analysis which leads to sufficiently good and safe results [2]. Such rules usually give procedures on tracking the indexes related to the quality of the element's used and on how to perform a proper response convergence study related to a varying meshing size.

For very simple structures with regular geometries (like isolated plates), the numerical results from the discrete problem can be benchmarked against exactly derived analytical solutions for the problem related to the continuum domain, which contain the same assumptions related to the physics of the simulation (therefore both numerical and analytical models would carry the same model-form errors). By doing this, the set of assumptions related to the discretization of the domain can be verified and the solution approximation error appreciated and set to an acceptable value.

Unfortunately, that is not the case for more complex problems as in the case of a submarine's compartment global collapse evaluation. In most situations for real-life problems, the exact analytical solution cannot be defined and the question if the numerical finite element model is representing the actual structure with enough accuracy remains.

It is reasonable to assume that the exact result of a problem simulated using numerical analysis will lay somewhere within the range of possible outcomes obtained while exploring the space of reasonably correct model parameters. Even if the such statement is not completely true, by the identification of a set of possible outcomes from different models, a quantification on the possible variability in the numerical results in current industrial practice can be determined. This quantified variability can bring important intuition on the accuracy of the finite element method for a determined problem and can put design rules involving safety factors or comparisons between numerical and analytical results into a different perspective.

Of course, such variability is very problem dependent, and a subset of all possible structural design space must be determined as the support for this investigation. In order to be in accordance to the context as laid out in the Introduction of this research thesis, the structural problem to be used as background for this research is the global collapse of a geometrically defined submarine's compartment.

From the above arguments, the following question can be formulated as the one to drive the efforts for the research of this thesis:

How much deterministic variation is expected in the global failure capacity of one typical submarine compartment obtained from different NLFEM modelling approaches?

It is important here to highlight the word "deterministic" of the above question. For sure every physical input in an analysis is in reality a stochastic parameter with a value which characterises it and a probability distribution, but this source of uncertainty is not explored in the present work.

From the geometric characteristics of the problem only shell type elements will be studied. Also, the work will focus on the behaviour of the structure up to the moment it reaches its maximum loading condition prior to instability, therefore the post-critical behaviour is not of interest here.

3 Theoretical Background and Literature Review

3.1. The Finite Element Method

As mentioned in the Problem Statement, the Finite Element Method is a strategy to solve differential equations which govern a behaviour of a continuous domain by approximating it using a defined quantity of elements with finite dimension. It was first used only for solid mechanics problems but currently it is the methodology of choice for a myriad of physical problems such as heat transfer, fluids, etc.

In the context of static structures (as in the case of this research), the basic differential equation from continuum mechanics being solved are of three types:

- Equilibrium Equations:

Those are the equations which arise from Newton's second law. Those are the ones which typically lead to the equations of motion. When dynamics are considered, it states that mass times acceleration must be equal to the resultant forces, meaning that stresses and body forces are related. But in the context of statics, it can be simplified into:

$$F = 0 \quad (3.1)$$

Where F represents the resultant forces within a domain. As an example, in the case of a two-dimensional problem with only external forces in a plane stress modelling approach (valid for thin objects, where transversal stresses can be neglected), this means that at any point in the domain the following relations must be respected [5]:

$$\frac{\partial \tau_{xx}}{\partial x} + \frac{\partial \tau_{yx}}{\partial y} = 0 \quad (3.2)$$

$$\frac{\partial \tau_{yx}}{\partial x} + \frac{\partial \tau_{yy}}{\partial y} = 0 \quad (3.3)$$

$$\tau_{yx} = \tau_{xy} \quad (3.4)$$

Where τ_{xx} , τ_{yy} , τ_{xy} and τ_{yx} are normal and shear stresses oriented in x and y directions.

- Compatibility Equations (Strain-Displacement Equations):

This is the set of equations which enforce the required kinematic relations between particles. The strains within a domain are determined by how different parts of the material displace between themselves. As an example, the compatibility equations for a plane stress problem, where higher order terms of the kinematic relationship have been dropped, are the ones below [5] (for a three dimension problem they would have the same form, just with more terms):

$$\varepsilon_{xx} = \frac{\partial u}{\partial x} \quad (3.5)$$

$$\varepsilon_{yy} = \frac{\partial v}{\partial y} \quad (3.6)$$

$$\gamma_{xy} = \frac{\partial u}{\partial y} + \frac{\partial v}{\partial x} \quad (3.7)$$

Where ε_{xx} , ε_{yy} and γ_{xy} are normal and shear strains and u , v are the field displacements in x and y directions respectively.

- Constitutive Equations (Stress-Strain relations):

Those equations represent the fact that the stresses in a material are determined by the strains. This statement considers that all intermolecular and atomic bonds present in the material's micro scale can be lumped into well-defined empirically based parameters to be used in the dimensional scale of structural problems. Here is where the Young's modulus and the Poisson's ratio are defined. For plane stress problems, those equations are the ones below:

$$\begin{bmatrix} \tau_{xx} \\ \tau_{yy} \\ \tau_{xy} \end{bmatrix} = \frac{E}{1-\nu^2} \begin{bmatrix} 1 & \nu & 0 \\ \nu & 1 & 0 \\ 0 & 0 & (1-\nu)/2 \end{bmatrix} \begin{bmatrix} \varepsilon_{xx} \\ \varepsilon_{yy} \\ \gamma_{xy} \end{bmatrix} \quad (3.8)$$

Where, E is the Young's modulus and ν is the Poisson's ratio.

Those basic equations can then be worked with and merged in different manners to generate a framework for a structural analysis, often using energy conservation methods. From those, the Virtual Work Principle is the most used for structural problems.

Such Principle states that increments in strain times the summation of internal stresses (Internal work) will equal the summation of the external loads times the increment in boundary displacements (External work). Within the internal work calculation, the *Constitutive Equations* are used to convert virtual incremental strains into incremental stresses, so that the Internal work depends only on the virtual incremental field of displacements (which can be assumed as dependent on the boundary displacements). The Virtual Work Statement contains the use of the *Compatibility Equations* (i.e. the increments in strain are related to the increments in displacement) and the *Equilibrium Equations* (i.e. the internal stresses are in equilibrium with the external loads), so that all three basic equations are considered.

The Finite element method advances by using the set of equations above in "natural" or "basis" elements (with unitary dimensions) and relating this natural element to every actual element of a discretized domain. Each actual element will have its own shape which relates to the basis element using maps called shape functions or interpolation functions.

For every node of an actual element, global displacements degrees of freedom are associated, so adjacent elements share the same displacement in some nodes. A stiffness matrix is defined for every element by making use of the virtual work principle to obtain how displacements and external loading are related. This is done using integration (e.g. see equation (3.9)) which requires functions to interpolate the displacements within the nodes of an element. If the same shape functions used for the shape interpolation are also used to interpolate displacements, the element is called an isoparametric element.

All element's stiffness matrixes are organized node-wise and orientation-wise in order to generate one global stiffness matrix \mathbf{K} which globally relates the nodal forces \mathbf{R} and the displacement's degrees of freedom \mathbf{U} in the general form $\mathbf{KU} = \mathbf{R}$. After solving for the displacements, post-processing techniques are applied to derive further quantities like stresses; strains and strain-energy.

For a non-linear finite element analysis, the procedures above are performed for step-wise and incrementally applied external loads and/or displacements. At each step the stiffness matrix can be updated to a tangent stiffness matrix ${}^t\mathbf{K}$ dependent on how the previous displacements and internal loads changed the characteristic of the problem both from geometry and material perspective. The load increments can be defined by analysing the residual errors calculated at the end of each step. The analysis is finished when a certain convergence criterion is met or when a numerical solution is no longer possible.

3.2. Types of Errors in Finite Element Method

In general, the uncertainties existent in the Finite Element Modelling results arise from the errors that a determined modelling approach has when related to the real phenomenon being modelled. According to Mahadevan [6] the errors in the predictions of a computational model are separated in the model form error and the solution approximation error.

The model form error arises from the incapacity of the selected model to completely represent the real phenomenon. It is in this type of error where the assumptions related to the physics of the problem will manifest themselves. Intuitively the identification of the model form error arises when one asks himself "Did I choose the correct equation?". This type of errors includes for instance the following aspects:

- use of small or large deformations assumptions;
- elasticity versus plasticity considerations;
- boundary conditions behaviour;
- initial out-of-circularity used in the analysis;
- the defined geometry to be analysed

The quantification of model form errors can only be made by proper verification experiments. From the list above, the parameter which seems the most likely to be set by the analyst's judgement is the use of small or large deformations (the others are often given as input for a given problem). The reader is referenced to [7] and [8] for more information in this type of error.

In the other hand, the solution approximation error is now related to the answer for the question: "Did I solve the equation correctly?". It usually relates to the differences between numerically solving the equation and the exact analytical solution which could exist for a determined problem. For example, this type of error is related to the aspects below:

- continuum versus discretized domain;
- meshing;
- order of the interpolation functions used;
- solver;
- integration scheme (both in plane and out of plane);
- time stepping in the analysis;
- convergence criterion

In this aspect the results can be improved by a proper meshing and with the proper assumptions on the mathematics of the problem. The quantification of the magnitude of the solution approximation errors is made from verification studies. In this document it is shown that for the case studied the three parameters which affect the analysis the most are the meshing, the order of the interpolation function used and the large deflections assumption.

3.3. Meshing and Mesh Size

Mesh and meshing are concepts which can be naturally intuited, but that can be quite tricky when one tries to lay a formal definition. Frey [3] brings the formal definition in the context of finite element analysis as:

*“A mesh is a covering-up of a given domain
defined, in most of the applications, via a given discretization of its boundary,
this covering-up being composed of possibly non simplicial elements”*

being simplicial elements, in a 2-D domain, connected closed sets of triangles.

Meshing can then be understood as the act of generating such a covering-up by subdividing a continuous geometric space into elements or cells. The geometric space is reconfigured for numeric analysis into a discrete number of simplified entities.

Many Meshing methods exist. Frey [3] provides them a general classification as the following: Manual or semi-automatic; Parameterization (mapping); Domain decomposition; Point-insertion/element creation and Constructive methods. The last being the broader definition and most probably the one in most current practice since it merges meshes created from all other methods by the use of topological or geometric transformations.

All methods above can be used to generate two different types of meshes: Structured meshes (when they have a high ordering degree) and Unstructured meshes (when they do not). According to Frey [3], the last is the one most used in current finite element practices and provide an efficient alternative to structured meshes for finite element method use in irregular geometries. In the present study, due to the symmetry and the geometrical characteristic of the problem, structured meshes can be used.

Three methodologies can be used to generate meshes: Spatial decomposition; Advancing-front and the Delaunay methodology. The details of meshing procedures are not within the scope of this study, but deeper investigation on the details of methods such as the Advancing Front can bring a better intuition on the methodologies being currently implemented.

The advancing front method generates the mesh in an element-wise manner. For a two-dimensional domain, the process begins from the discretized boundaries as the first front (i.e. the set of mesh entities which splits the domain into meshed and not meshed) and advances by the materialization of new points and their connection to points existing in the current front to create elements. At each increment of the procedure, a new front is created within the domain until the complete covering up of the domain.

The discretization of the boundary is made such that it respects a size distribution function within the domain (provided by the user or constructed from input information). From the discretized boundaries optimal points are generated inside the domain. The optimal points are points which lead to equilateral triangles for two dimensions. The optimal point is located within the normal to the 2d front edge which intersects its mid-point. This location can be iteratively improved by optimization procedures. The distance from the edge to the optimal point is defined by the size function.

The size function for the element can be defined for each vertex of a control space (being control space in practice the specification of a function supported at the vertices of an a priori simpler background triangulation of the domain), or, for simpler domains, the element size function can be an analytical function defined over the entire domain. In order to simplify the analysis performed in this thesis, the size function will be set as a single real value for the entire domain. So, when the mesh size parameter is changed, it impacts the size function for the entire domain as a whole with one single value.

For the present study, the Mesher algorithm from the Ansys software package is used. The Mesher algorithm is a proprietary information from each software package and the internal nuances of each solution is only known by the company's developers. But, from the Ansys reference documentation available for

consultation on-line [9], it can be understood that Advancing Front method is used (probably aided with other methodologies for mesh improvements) when the “Advanced Size Function” capability of the program is set as OFF. The meshes of the present analysis will be constructed under this setting.

3.4. Shell Element Types and Order

The element order is the degree of the shape functions used to interpolate the discrete nodal position or displacements into the continuous positioning or displacement fields within the element.

Linear elements do not require intermediate nodes at the element’s boundaries for their shape functions definition (i.e. two points suffice for a line), but quadratic elements formulated with second order functions do require a node within the element’s edge (in this case three unknown coefficients to be solved for are present in a parabola’s equation).

According to the Ansys software [9] theory reference available on-line, both element types (linear and quadratic) can be used for structural analysis. The linear element will often yield a smaller computational time, but degenerate elements (i.e. triangular elements for the 2-D linear case) should be avoided in regions with large gradients in the responses. Also highly distorted elements should be avoided. Ansys manual also mentions that linear elements seem more suitable for non-linear finite elements usage.

In the case of degenerate elements, the quadratic formulation usually yields better results, but care should be taken when using quadratic elements in some situations. For example, in dynamic analysis such elements have a non-uniform mass distribution. Also, for more complex formulations like contact or gaps, the mid-side nodes will bring problematic aspects for the solver.

Within the Ansys Workbench software framework, linear shell elements are modelled by the element named SHELL181. In the present thesis, when any mention to linear element is made, it is referencing this element type. It has four nodes and has six degrees of freedom at each node (three translations and three rotations). From the loading aspect, it is an element well suited for the present analysis since it has capabilities to deal with the follower loading problem for distributed pressures [9] (Important for problems related to hydrostatic pressure being imposed on cylinder walls with out-of-circularity).

Linear plane elements are prone to the shear locking problem. SHELL181 handles that by assuming a shear strain formulation from Bathe-Dvorkin [10].

Within the same program framework, quadratic elements are simulated using the element SHELL281. Hereinafter, the denomination of quadratic element in this document is a reference to this type. It has six degrees of freedom at each node (again, three translations and three rotations), but now 8 nodes are present. This element also accounts for the follower loading problem. It is only suitable for thin to moderately thick shell (the through-thickness stress is zero). From being a quadratic element, shear-locking phenomenon does not manifest itself representatively.

3.5. Element's In Plane Integration Scheme

A crucial step for any finite element analysis procedure is the determination of the element's stiffness matrix. In the context of 3-D problems it is derived from an integration procedure which has the form [11]:

$$\mathbf{k} = \int_V \mathbf{B}^T \mathbf{E} \mathbf{B} dV \quad (3.9)$$

Where:

- \mathbf{k} is the element's stiffness matrix
- \mathbf{B} is a matrix which relates strains and displacements and is obtained by differentiation of the shape functions
- \mathbf{E} arises from the constitutive stress–strain relations
- V is the domain determined by the element's 3-D boundaries

This integration is evaluated numerically by the finite element's codes and for this mainly two procedures exist: the reduced or the full integration, both related to Gaussian Quadrature [12] rules. This methodology evaluates the integral by strategically weighting the function's value at determinate optimized coordinates and performing their summation. For the full in-plane integration procedure, typically four integration points from the quadrature rules are considered. In the other hand, for the reduced integration only one point located at the center of the element is taken into account.

Obviously, the full integration brings results with smaller numerical errors when compared to the reduced scheme, but in the context of 2-D structural non-linear problems this error can be beneficial. From the assumptions on the element's formulations, usually they have a stiffer response when compared to their actual behaviour. The small error in the reduced integration schemes alleviates this phenomenon and approximates the results to the real responses.

It should be observed however that for some specific cases the reduced integration can lead to the stiffness matrix to be null and numerical instabilities can arise [13]. The spurious solutions which can be obtained from this issue are called hour-glass modes.

3.6. Position and Number of Integration Points Through the Thickness

To correctly simulate the bending behaviour of a shell element, use is made of the through-thickness integration points in the determination of the stiffness matrix. If only one integration point is considered, the in plane bending stiffness cannot be defined, and the element behaves as a membrane (only the planar stiffness exists).

For plane elements with elastic material behaviour, two integration points at the surfaces of the elements would suffice, since the stress distribution along the thickness can be approximated as linear. But, if material plasticity is considered, discontinuities will be present in the stress and strain curves through the element thickness and additional integrations points are required to properly define their distributions. For the Ansys' elements used, the integration points are located in accordance Simpson's integration rule [9] but positioned in a non-standard manner (two nodes always located at the top and bottom surfaces). Any odd numbers quantity of points is possible, being 5 the standard minimum quantity for non-linear materials bending quantification.

Obviously, the larger the quantity of integration points, the larger the accuracy of the results but also the larger the computation time.

3.7. Geometrical Nonlinearities and Large Deflections

The consideration of “large deflections” means that geometrical non-linearities are included in the analysis. Mathematically this implies that the second order terms of the basic equations will not be neglected [9] and that the stiffness of the structure changes as it deflects.

Within the finite element framework, the consequence of this is that the strain components require complete expressions for their definition [14] and changes in the position, orientation or shape of the elements must be accounted for during the iterative procedures since now the stiffness is a function of the displacements.

The changes in geometry are accounted for by updating the tangential stiffness matrix at each step. In ANSYS [9] four types of geometrical non-linearities exist. They are listed below:

- Large strain – If considered, the assumption is that strains are finite. Therefore, changes in the element’s shapes (e.g. cross section) are contemplated in the analysis.
- Large rotation – If considered, the assumption is that rotations are large and not negligible. The strains which leads to stresses are assumed as small and considered by means of linear expressions. Changes in shape are not considered, but rigid body motion is contemplated.
- Stress stiffening - If considered, the assumption is that strains and rotations are small. Rotations are considered with a first order approximation.
- Spin softening - If considered, the assumption is again that strains and rotations are small. It is related to the dynamics relating the transverse vibrational motion and the centrifugal force which arise due to an angular velocity.

Of large interest here is the stress stiffening effect. This is the stiffening (or softening) of the structure due to its stress state. The matrix which contemplates this effect is called the stress stiffness matrix and is added to the regular stiffness matrix to give the complete stiffness of the problem. It is the stress stiffness matrix which is used in the perturbation analysis for the eigenvalue buckling evaluation.

In the present study, the necessity for the consideration or not of the large displacements in the analysis can be quite doubtful. As it is shown on the results chapter, at the verge of collapse the displacements are small.

3.8. User’s Level of Expertise

In this thesis, the variability of the results as function of the level of expertise of the analyst performing a Finite Element Model is also explored. In this context it is important to have a framework which allows for a proper classification of possible users. For this, some knowledge can be borrowed from the field of Task Analysis and Interface Design. From that field, according to Hackos and Redish [15], four levels of expertise can be defined:

- Novices: Users which are completely new for a product
- Advanced beginners: Users who have their main goal as to have the task finished
- Competent performers: Users who can perform more complex tasks within and activity
- Expert performers: Users who have a comprehensive theoretical understanding not only on the activity to be performed but also on the whole system involved in the problem.

In this research, it will be considered that complete Novices would not perform meaningful Finite Element Analysis results which could be present in the industry. So only the last three classification are explored.

In general, it will be considered here that the experience and knowledge of the analyst will play a role on the selection of the parameters to be used and the range of parameters which could be included in the analysis. This means that Beginners will have a much larger space of possible parameter settings then Expert performers, who would know upfront some possibilities which can be dropped from the analysis by deviating much from both the theory and the physics of the problem.

3.9. Similar Studies from Other Authors

The research performed by other authors bring important contribution to the results for this thesis in terms of being a basis for comparison on the obtained variability quantification.

On the proceedings of the 19th International Ship and Offshore Structures Congress, held in 2015 two benchmark studies are presented [1]. The first study evaluates the different results which ten different finite element (FE) analysts obtained for a same defined problem of a bent box girder which had experimental results available. The second study is focused on the effects that initial imperfection and lateral loads have on the global capacity of the hull of a bulk carrier.

The first study presented in 2015 has great similarities to the present thesis research. It also explores possible solution approximation errors of a plate-like stiffened compartment by allowing the analysis to set their own modelling strategies for a given structural problem with well-defined inputs. All ten analysts used the same geometry, plasticity characteristics, initial imperfection and boundary conditions, but could select their own approach by choosing the solver, software, meshing and element type. Although the benchmark study demonstrated that there is a large difference between the experimental results and the NLFEM predictions, the results from all analysts presented a nice correlation. From the population of the results, uncertainty on the predictions were calculated as varying from 3.3% to 10.6%. This uncertainty is shown in the references to be related in value to the ones provided by the International Association of Classification Societies - Common Structural Rules (IACS-CSR) partial safety factor. Other important finding presented in that study is that the results were insensitive to the initial imperfections magnitude. The reasoning explained there is that a small initial imperfection is enough to initiate the buckling nucleation and trigger the instability.

The second study is less related to the present thesis, since it explores global behaviour of an entire carrier and the four participants had larger freedom on preparing their models related to boundary conditions and extend of the region modelled for the response of interest. Anyway, the results obtained for the Hull girder ultimate strength had an uncertainty ranging from 6.44% to 16.35%. This uncertainty was obtained from a much smaller population of results but is still somewhat close to the values of the previous paragraph. This benchmark study concluded that the NLFEM results are in good agreement to the predicted value from the IACS-CSR.

On the proceedings of the same congress, but now in 2018, two other benchmark studies are again presented. The first one is related to frame-like structures subjected to fire loading, which has little relation to the present research and will not be commented. The second study revisits the same bent box girder analysed in 2015 and extends the analysis with the test rig's structure included in the model. This is made with the intention of increasing the adherence between the results from the experiment and the NLFEM models by better simulating the boundary conditions at the imposed moments location. For this case seven different analysis had larger freedom to select all model parameters including exact degrees of freedom, mesh size, solver, imperfections, residual stresses and material. From this, the results obtained by each analyst in their simulation lost the excellent correlation which was obtained in 2015 and now uncertainties between 15.13% to 22.7% appeared.

4 Methodological Approach

As mentioned in the Introduction, this thesis aims in quantifying possible variability in Finite Element Analysis results. That is done by capturing a set of responses at determinate characteristic locations (related to structural failure) of a single mechanical problem solved by the use of different strategies for setting the modelling parameters (and therefore with different model forms and solution approximation methods). The set of different results is then grouped into subsets associated to possible user's expertise and used as input to derive statistical parameters related to uncertainty. That brings intuition on how much variability can be expected, for each user level of expertise, in the resolution of a mechanical problem similar to the one here presented, using the Finite Element Method.

The mechanical problem that will serve as the background for the study is the obtention of the value for the hydrostatic pressure which leads to the failure of the midship section of the hull of a Manatee class submarine. Details related to the mechanical input aspects are presented on chapters 4.1 and 4.3 below.

The assumptions on how to account for the possible failure modes (and therefore which are the responses of interest) are explained on chapter 4.7.

4.1. Reference Geometry

4.1.1. The Manatee Class

The Manatee Class submarine has an operational diving depth is of 250m (external hydrostatic pressure of around $\sim 2.5\text{MPa}$). As it can be perceived by the results demonstrated in chapter 5, this defined value is far below critical.

Figure 1 below (taken from [16]) brings an overview of the pressure vessel and highlights the region which is used as subject for the present research.

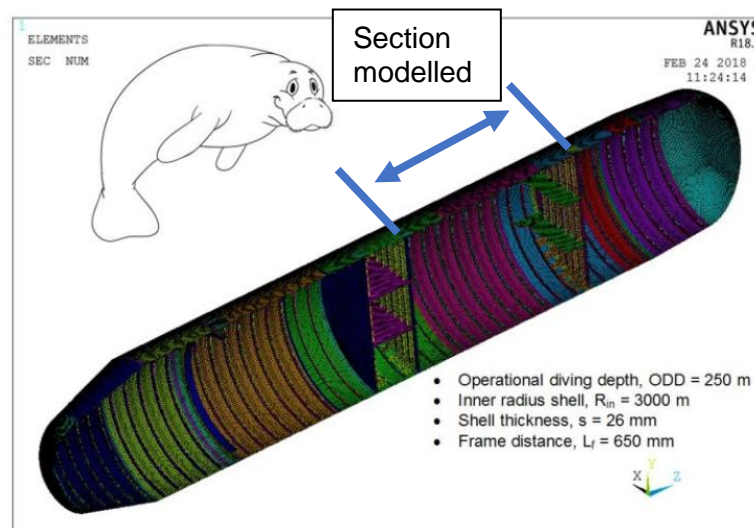


Figure 1 - Overview of the Manatee class pressure hull

4.1.2. Detailed Geometry Modelled and Out-of-Circularity

The general information related to geometry is listed below and shown in Figure 2, extracted from [16]:

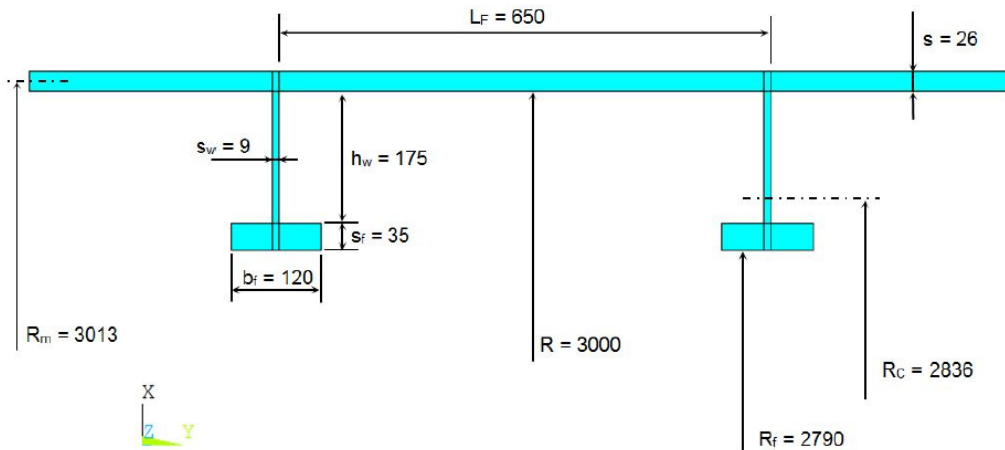


Figure 2 - Dimensions of the Manatee Class Pressure Hull

The domain of the model comprises the region in between bulk heads (See Figure 1), and includes in total 12 repetitions of interframe spacings, with a total length of 7.8m. Figure 3 brings an overall view of the region considered:

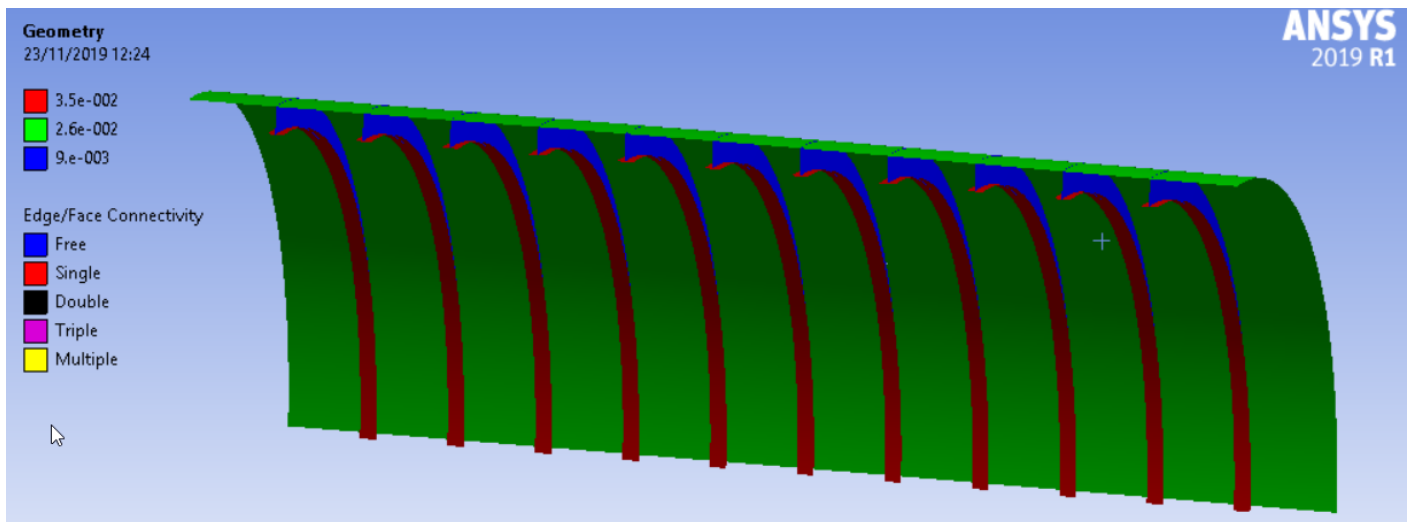


Figure 3 – Overview of the FE model

To trigger the non-linear failure phenomenon, an initial imperfection is required. According to [17], a suitable out-of-circularity for the problem with amplitude of $0.005 \cdot R$ should be used to satisfy common rules from classification societies [18]. The imperfect shape of global modes is related to fabrication processes and, can present itself in many forms. For this study, and imperfect shape with four waves around the circumference is assumed. The imperfect shape used in the analysis is obtained by directly translating the geometry of the surfaces modelled in order to match the assumed waves.

Figure 4 below illustrates the imperfect shape assumed for the non-linear analysis.

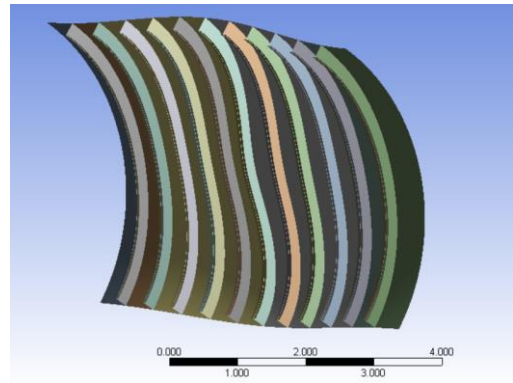
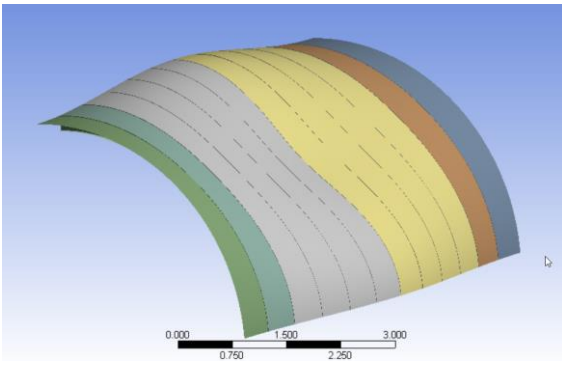


Figure 4 – Imperfect shape (amplified 20x)

From the shape of the imperfection assumed, it is possible to exploit symmetry (see chapter 4.3.3) and largely reduce the size of the model.

The geometry above and the modelling parameters in chapter 4.3 are kept the same for all models listed in chapter 4.4

4.2. Axis Convention and Coordinate System

The problem is approached using the Cartesian coordinate system, where the “x” axis represents the longitudinal direction. Figure 5 below demonstrates the system used.

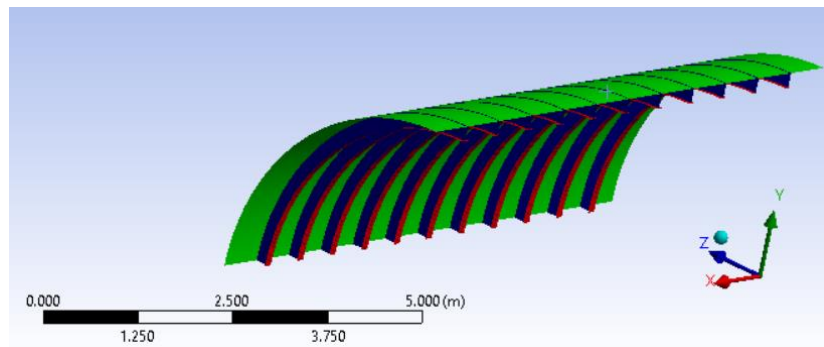


Figure 5 – Coordinate System

4.3. General Modelling Parameters

This chapter presents the values and modelling assumptions used to construct the model that is the background of this research.

4.3.1. Material

- Material = Steel Grade HY80
- Young’s modulus, $E = 206000$ MPa
- Poisson ratio, $\nu = 0.30$
- Yield stress = 552 MPa

The material is considered as an elastic-perfectly plastic material with isotropic hardening. The tangent modulus for the plastic plateau is set to zero. Figure 6 below demonstrates the material curve adopted.

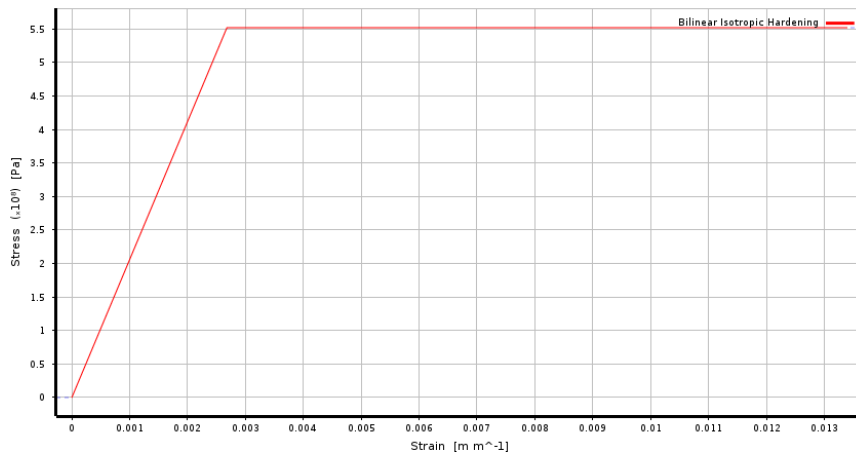


Figure 6 – HY80 material curve considered

4.3.2. Loading

The hydrostatic external pressure is applied as 10Mpa, related to a submergence of 1000m (a magnitude which ensures that failure will be reached). The radial pressure is imposed as constant pressure perpendicular to the faces in the model. The follower force effect is accounted for in the analysis cases where the large deflection assumption is considered (see chapter 4.4 for the model types which have this consideration). The pressure is applied at the elements in red in Figure 7 below:

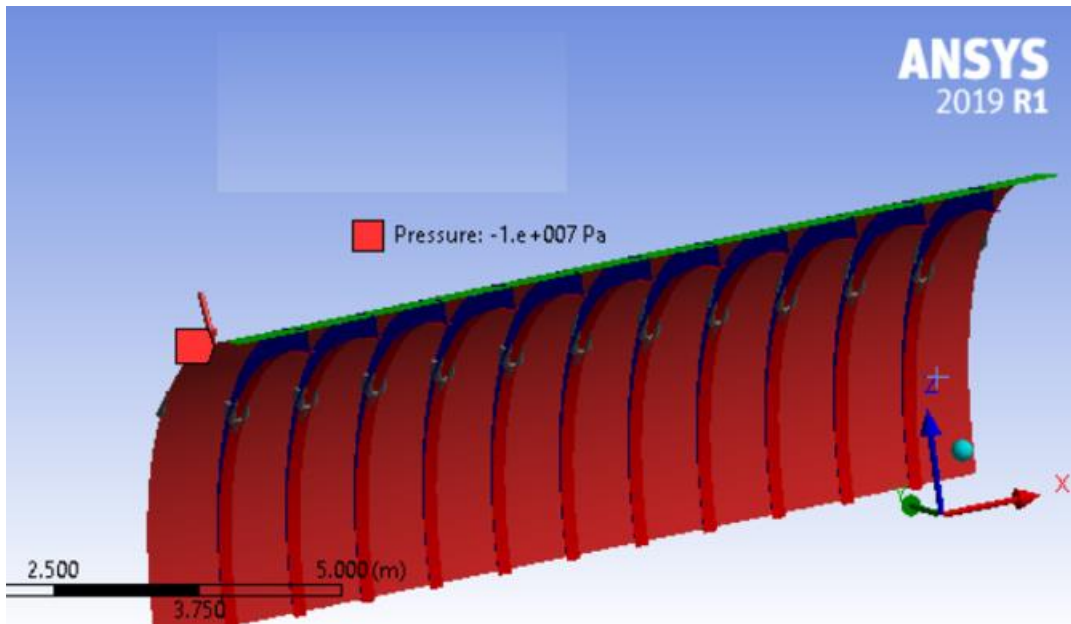


Figure 7 – Application of external hydrostatic pressure of 10Mpa

And the longitudinal forces which arise at the extremities of the model are modelled as a force imposed at a remote node which constrains in the longitudinal direction the external longitudinal edge of the model. The value of the force applied is of 71.3kN as shown on Figure 8 below:

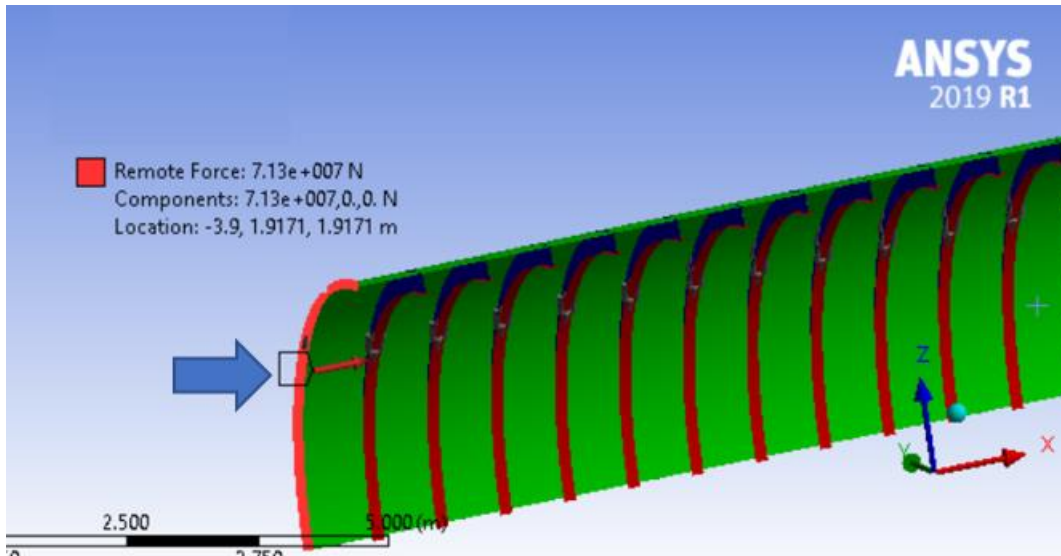


Figure 8 – Longitudinal force of 71.3kN

4.3.3. Boundary Conditions

The boundary conditions for the model are a composition of symmetries, fixed displacements and coupling at the force location, as illustrated in Figure 9 to Figure 12 below:

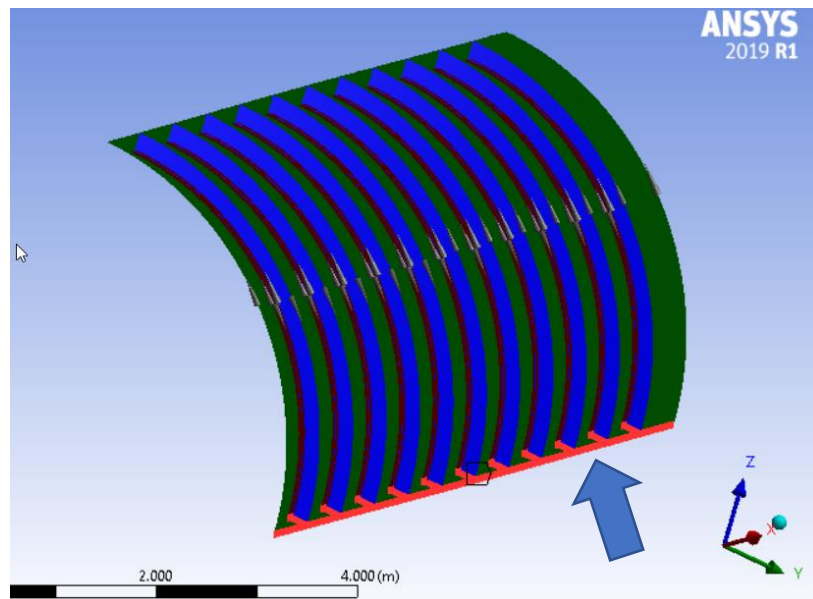


Figure 9 – Symmetry over z axis (affected edges in red)

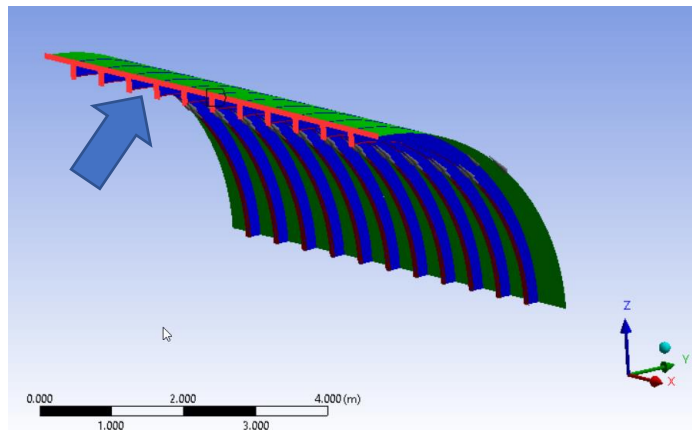


Figure 10 – Symmetry over y axis (affected edges in red)

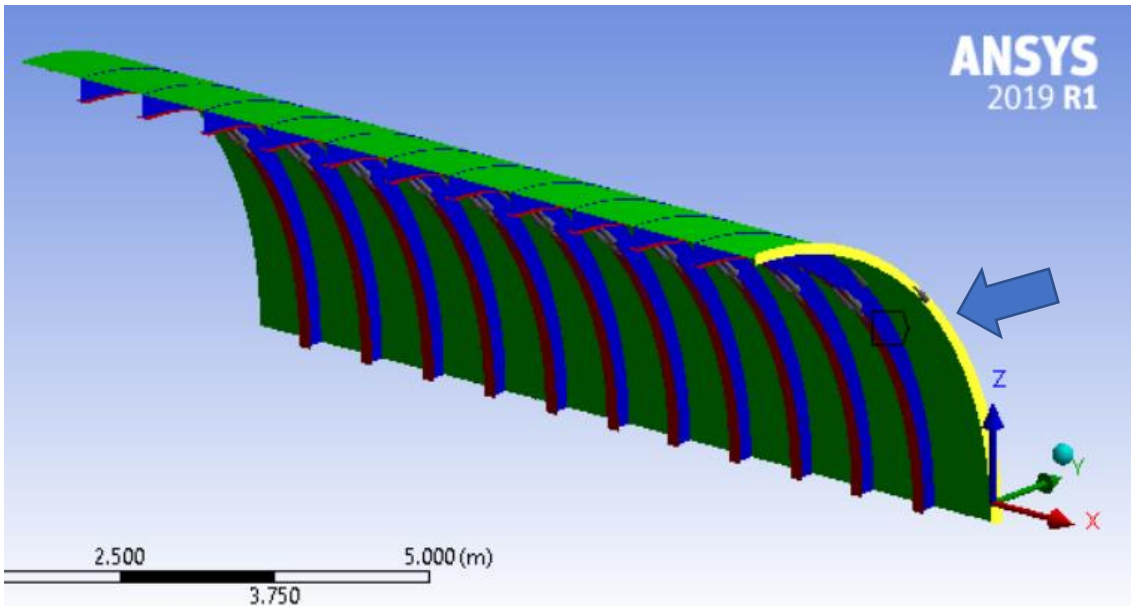


Figure 11 – Rigid support both for translations and rotations (affected edges in yellow)

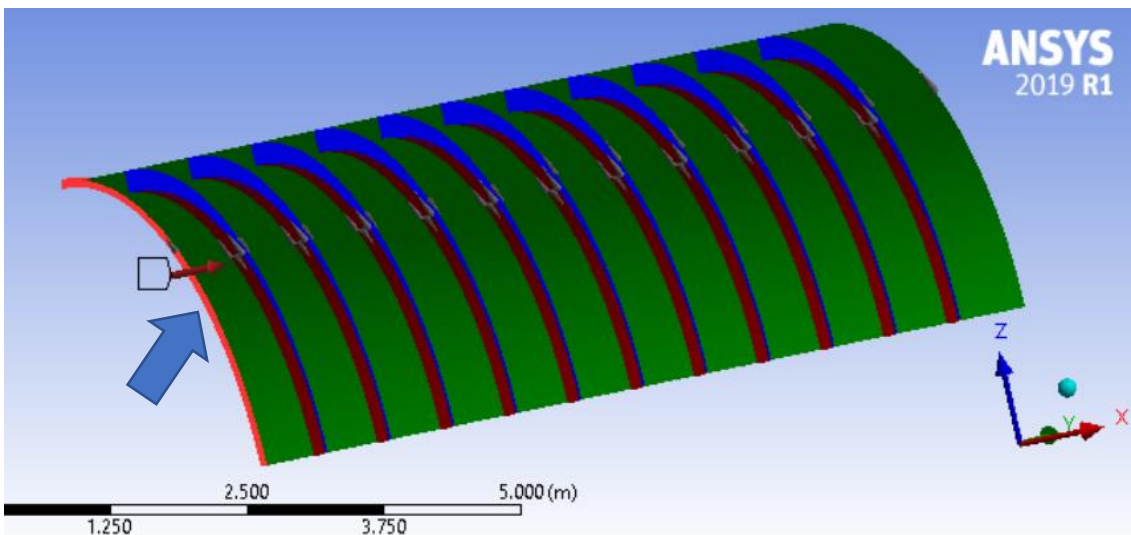


Figure 12 – Rigid support at load application edge (only translation in “x” is allowed). All nodes at the edge are coupled for translation in “x”

4.3.4. Linear Elements Near the Bulkheads

To simulate the effect of the reinforced region near the bulkheads, and to ensure that the stress concentrations and peaks which occur at the vicinity of the longitudinal edges of the model will not impact the captured results, some regions of the model have the material non-linear effects suppressed. Those regions are illustrated in darker grey in Figure 13 below.

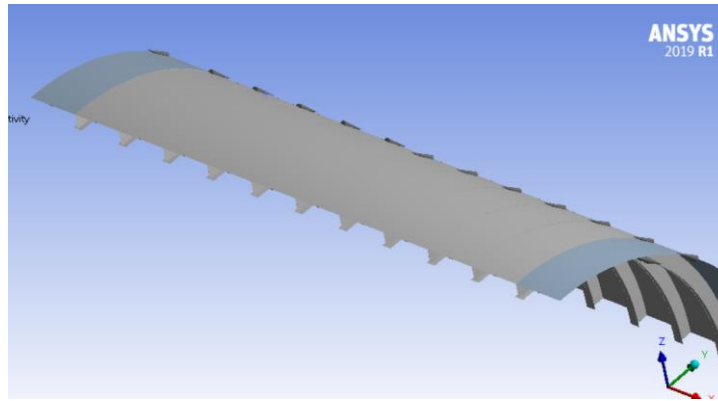


Figure 13 - Regions at the hull with elastic material (in darker grey)

The idea is that by suppressing the yield of those elements, the plasticity effects are forced to arise at the centre of the model, near the regions where the out-of-circularity have its peaks. In reality, the reinforcements near the bulkheads ensures that this is the expected behaviour.

4.3.5. Meshing

In this study, several mesh sizes will be considered as it is explained in chapter 4.4. The meshes vary from a very fine (with 20 elements present in the interframe distance - Figure 14), to a very coarse (with only 3 elements discretizing the interframe span - Figure 15).

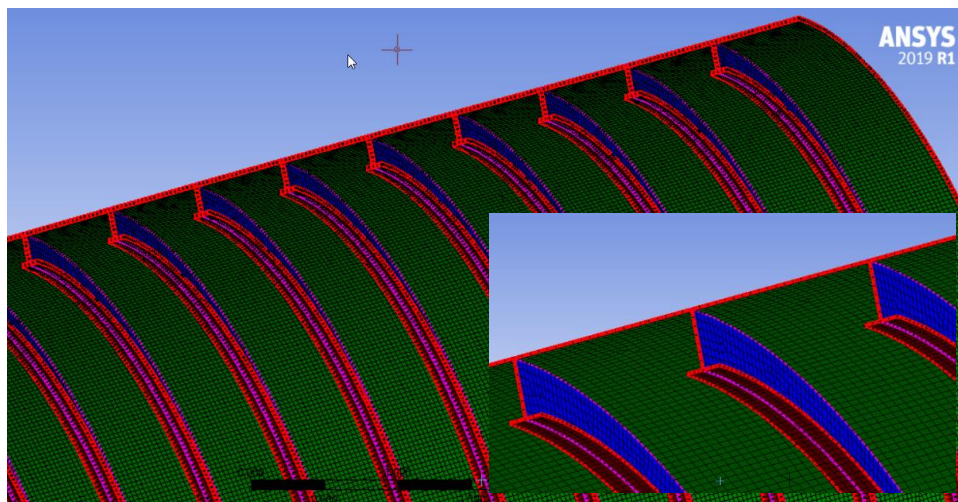


Figure 14 - Very fine mesh (20 elements interframe)

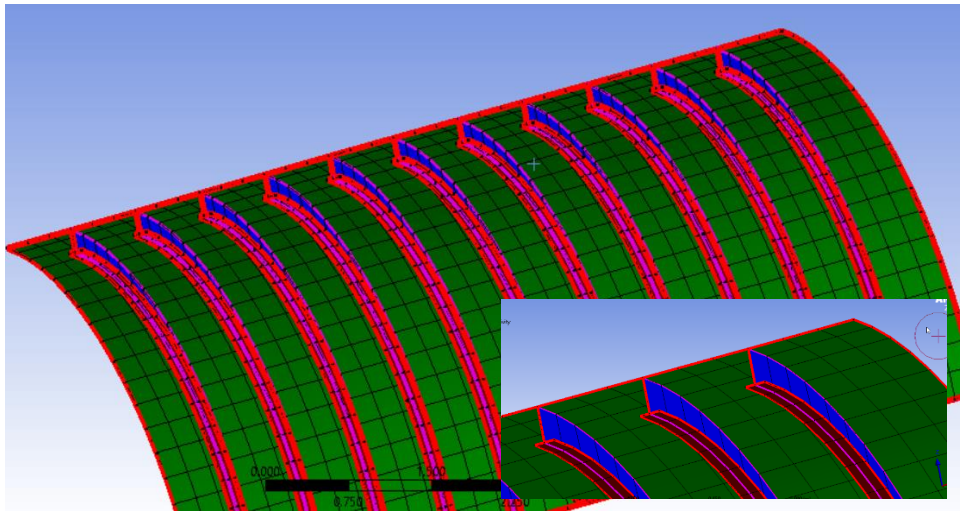


Figure 15 - Very coarse mesh (3 elements interframe)

4.4. Identification of the Constructed Models

The key parameters explored in this study as source of uncertainty are:

- Mesh size;
- Order of the shell elements;
- In plane integration scheme;
- Large Deflections consideration.

Those are parameters for which typically the analyst will go through a decision process on how to set them and which might *a priori* greatly impact the Model results.

To explore the space of possibilities, six model types are defined in the framework of this study. The model types are shown at Table 1 below:

Table 1 - Model Types

| Model Type | Element Order | Large Displ. | Integration Scheme |
|------------|---------------|--------------|--------------------|
| 1 | Quadratic | Off | Full |
| 2 | Linear | Off | Reduced |
| 3 | Linear | Off | Full |
| 4 | Quadratic | On | Full |
| 5 | Linear | On | Reduced |
| 6 | Linear | On | Full |

Then, for each model type, a range of five possible mesh sizes are considered from very coarse to very fine. Table 2 below describes the meshing size consideration:

Table 2 – Mesh Classification

| Mesh Classification | Mesh Size [m] | Number of elements between frames |
|---------------------|---------------|-----------------------------------|
| Very Coarse | 0.216 | 3 |
| Coarse | 0.13 | 5 |
| Reasonable | 0.065 | 10 |
| Fine | 0.04167 | 15 |
| Very Fine | 0.0325 | 20 |

4.5. Arrangement of The Parameters for Each Level of Expertise

As mentioned on chapter 3.8, the experience of the user plays a role on how wide the variability of possible parameters can be.

When selecting the mesh sizes, Competent and Expert performers will for sure perform a mesh convergence study and only the meshes which presented a converged result for the tracked responses (in our case Von Mises stresses and Linear Buckling pressures) would be used. In this study it is considered that Advanced Beginner users could use incorrect mesh sizes, or mesh sizes which are just the default values in the Finite Element Program, so the entire range of mesh sizes from this study is included in their set.

In chapter 5.4 the mesh convergence studies are shown and it is identified that the mesh sizes from 0.0325m to 0.065m have converged results for the presented parameters and are the ones selected as representing the Competent and Expert performer's choice.

For the element order, again the Advanced beginner would use the default option (so both quadratic and linear elements could be used). It is possible that Competent Performer would select quadratic elements aiming at a better precision, but also that they would take into consideration the text in Ansys manual where it is written [9]:

“...A quadratic element has no more integration points than a linear element. For this reason, linear elements will usually be preferred for nonlinear analyses”

So, the entire range of possibilities for the element order's selection is considered for Advanced Beginners and Competent Performers.

In the other hand, Expert users would have enough experience and knowledge in the specific type of problem studied in this thesis (or would perform enough verification exercises) to make the choice for the use of only quadratic elements. In the context of this thesis, the reasoning for such selection would be three: (1) Quadratic elements present a much better convergence behaviour - see chapter 5.4; (2) In the verification process described in chapter 4.6 quadratic elements were used in order to match the analytical results; (3) Quadratic elements presented the expected first yield location (at stiffener) already with a reasonably sized mesh, while linear elements required very fine meshes – see chapter 4.6 - Table 4

In relation to the in-plane integration scheme, it is considered in this research that Advanced Beginners could be prone to use whichever is the standard setting for this parameter in the software or not completely evaluate the impact of its variation. Some Competent Performers would be aware of the better accuracy from the full integration, but others would also take into consideration the possible excessive stiffness (and the benefits which arise from the small softening present in the reduced integration). So, both full and reduced in-plane integration schemes are present in the set of results related to those expertise levels. In the context of an analysis performed using Ansys, Expert users would use the full integration scheme, since it is the only available option when quadratic elements are used.

Finally, when considering turning on the Large Displacements option, the Advanced Beginner would select the default (off). The Competent Performer could judge the displacements of the model to be small in relation to the hull's thickness. To illustrate this, Figure 16 below demonstrates that the hull's deflection at the condition when a typical non-linear model of this research reaches yield at midbay is of only 9.7mm

(only 0.12% of the total distance between bulkheads). From this, it is assumed that the Competent Performers could have both options (on or off) for the large displacements setting.

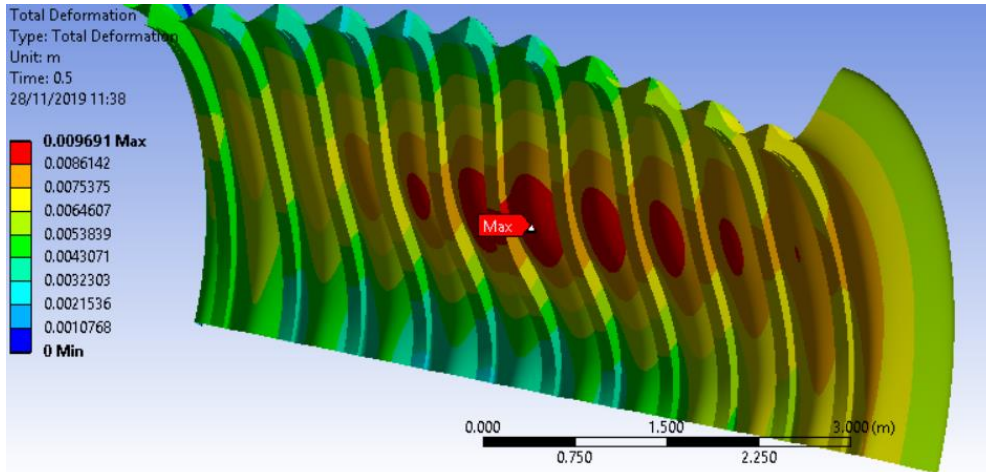


Figure 16 - Maximum displacement when a typical model reaches yield at midbay

But the Expert Performer would be aware of the necessity of considering the geometrical non-linearities which develop during the loading process in a full-non linear model used to evaluate collapse (both to consider the geometrical and following force effects), and for sure would have the Large Displacements option turned on for the analysis.

Table 3 below summarizes the reasoning above for each level of expertise considered.

Table 3 – Model parameters for each Level of Expertise

| Model Type | Mesh size (m) | Element Order | Large Displ. | Integration Scheme | Adv. Beginner | Competent performers | Expert performers |
|-----------------------------------|---------------|---------------|--------------|--------------------|---------------|----------------------|-------------------|
| 1 | 0.216 | Quadratic | Off | Full | x | | |
| 2 | 0.216 | Linear | Off | Reduced | x | | |
| 3 | 0.216 | Linear | Off | Full | x | | |
| 4 | 0.216 | Quadratic | On | Full | x | | |
| 5 | 0.216 | Linear | On | Reduced | x | | |
| 6 | 0.216 | Linear | On | Full | x | | |
| 1 | 0.13 | Quadratic | Off | Full | x | | |
| 2 | 0.13 | Linear | Off | Reduced | x | | |
| 3 | 0.13 | Linear | Off | Full | x | | |
| 4 | 0.13 | Quadratic | On | Full | x | | |
| 5 | 0.13 | Linear | On | Reduced | x | | |
| 6 | 0.13 | Linear | On | Full | x | | |
| 1 | 0.065 | Quadratic | Off | Full | x | x | |
| 2 | 0.065 | Linear | Off | Reduced | x | x | |
| 3 | 0.065 | Linear | Off | Full | x | x | |
| 4 | 0.065 | Quadratic | On | Full | x | x | x |
| 5 | 0.065 | Linear | On | Reduced | x | x | |
| 6 | 0.065 | Linear | On | Full | x | x | |
| 1 | 0.416 | Quadratic | Off | Full | x | x | |
| 2 | 0.416 | Linear | Off | Reduced | x | x | |
| 3 | 0.416 | Linear | Off | Full | x | x | |
| 4 | 0.416 | Quadratic | On | Full | x | x | x |
| 5 | 0.416 | Linear | On | Reduced | x | x | |
| 6 | 0.416 | Linear | On | Full | x | x | |
| 1 | 0.325 | Quadratic | Off | Full | x | x | |
| 2 | 0.325 | Linear | Off | Reduced | x | x | |
| 3 | 0.325 | Linear | Off | Full | x | x | |
| 4 | 0.325 | Quadratic | On | Full | x | x | x |
| 5 | 0.325 | Linear | On | Reduced | x | x | |
| 6 | 0.325 | Linear | On | Full | x | x | |
| Quantity of models for each level | | | | | 30 | 18 | 3 |

4.6. Verification of Models

In order to ensure the correctness of the models used in this research, a verification exercise was performed for a simpler version of the model which did not include the out-of-circularity nor non-linear effects. The results from this model were compared to the results obtained from available analytical formulae for the problem and also compared to the results obtained by this thesis supervisor, who performed an independent modelling for the same problem. For this research, it is considered that the thesis supervisor is an Expert Performer.

Figure 17 below demonstrates the compared results of unaveraged axial stresses stress in the hull along a longitudinal path. The results from the thesis supervisor have the markings for which are the theoretical values obtained analytically.

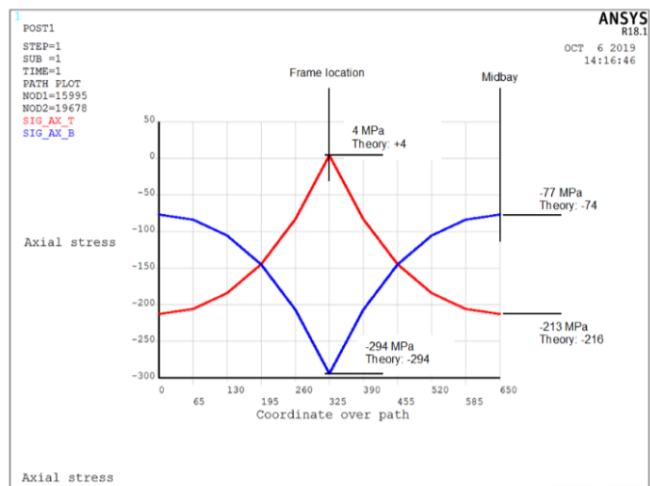
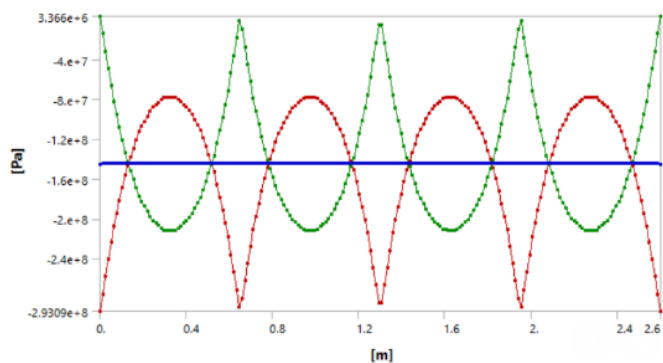


Figure 17 - Comparison for verification. Left - Results by the author; Right - Results by the thesis supervisor

The models which produced the same results as the analytical formulation were constructed using a reasonably refined mesh (element size around 0.065m) and quadratic elements. As described in chapter 4.5, those parameters are related to possible choices from Expert Users.

With this comparison exercise it was ensured that aspects presented in chapter 4.3 related to boundary conditions; loading; geometry; symmetry; physics are correctly simulated in the models used for this research. Also, from having matching results to analytical formulation for this simpler problem, the assumptions that the modelling parameters for element order (quadratic) and meshing (0.065m) were verified as being the suitable ones from an Expert Performer.

While verifying the results with the thesis supervisor - now in respect to models including non-linear effects and out-of-circularity - the author identified unexpected results from the numerical models which were not foreseen by the analytical formulations. The unexpected result is related to the sequence of the developments of the plastic hinges along the failure process. While the analytical formulations predict that the first location to yield is the inner fibre of the hull at the stiffener location, the author found that this situation for numerical models is actually parameter dependent and the locations of first yield happened in several different locations within the constructed models (but, for all model types, with a very fine mesh, the first yield at the stiffener location was obtained). Table 4 summarizes the obtained location of first yield per model type.

Table 4 – Location of first yield per model type and mesh size

| Mesh Size [m] | Model Type | Location of first yield at hull |
|---------------|------------|---|
| 0.13 | 1 | Interframe Midbay |
| 0.13 | 2 | Interframe Midbay |
| 0.13 | 3 | Interframe Midbay |
| 0.13 | 4 | Interframe Midbay |
| 0.13 | 5 | Interframe Midbay |
| 0.13 | 6 | Interframe Midbay |
| 0.065 | 1 | Stiffener |
| 0.065 | 2 | Interframe Midbay |
| 0.065 | 3 | Interframe Midbay |
| 0.065 | 4 | Interframe Midbay and Stiffener at same time step |
| 0.065 | 5 | Interframe Midbay |
| 0.065 | 6 | Interframe Midbay |
| 0.0416 | 1 | Stiffener |
| 0.0416 | 2 | Interframe Midbay and Stiffener at same time step |
| 0.0416 | 3 | Interframe Midbay and Stiffener at same time step |
| 0.0416 | 4 | Stiffener |
| 0.0416 | 5 | Interframe Midbay |
| 0.0416 | 6 | Interframe Midbay |
| 0.0325 | 1 | Stiffener |
| 0.0325 | 2 | Stiffener |
| 0.0325 | 3 | Stiffener |
| 0.0325 | 4 | Stiffener |
| 0.0325 | 5 | Stiffener |
| 0.0325 | 6 | Stiffener |

One reason for the above might be the singularities which exist at the stiffener location. Other cause might be the character of the first yield location as being function of the out-of-circularity considered, since in all models which were constructed in the condition without imperfections, the first yield always happened at the stiffener location (in accordance to the analytical expectations). The curious behaviour only manifested itself when out-of-circularities were considered.

4.7. Responses of Interest and Failure Criteria

The challenge here is to determine the parameters which can represent by means of simple scalar functionals the structural behaviour of each model in the model space investigated.

It is reasonable to assume that a main goal of a finite element analysis, in the context of a submarine`s hull design, is the identification of the external unbalanced hydrostatic pressure which would lead the hull`s structure to reach a defined Failure Criterion (an Ultimate Limit State - ULS). The above statement does not necessarily mean the collapse of the hull. It means just that an Ultimate Limit state for the hull`s structure is reached. Several criteria may exist for the Ultimate Limit State, but all would be related to the impossibility for the hull to be suitable for an increase on the loading (for example, further submergence would lead the hull to not fulfil its original function).

It is not within the scope of the present study the proper definition nor the debate of Ultimate Limit States which economically bring a minimally safe design. But usually the minimization of the hull plate`s thickness is a target for design, since it reduces the submarine`s mass and increases the payload, and slender configurations are obtained in most geometric arrangements. From this it can be expected that any structural evaluation would have to determine somehow the values of the pressures which would lead to the possibility of failure related to instabilities.

A possible procedure in current industrial FEA practice to assess instability is the obtention of the “Buckling resistance from non-linear analysis using standard defined equivalent tolerances” [1]. This method requires that the effects of residual stresses; deviations from the perfect geometry and material non-linearities are

considered in the full non-linear model by the use of suitable theoretical material inelastic curves and equivalent model imperfections. For such analysis it is reasonable to assume that the scalar quantities listed below would necessarily be involved in the capacity evaluation of a Submarine`s hull.

For all capacities below which are related to yielding, the criterion for the limit when plasticity start to develops is that it begins when the Von Mises stresses are reached.

Hydrostatic pressure which would lead to the first yield of any structural component of the model
(P_{1st_yield})

In the case that a very conservative safety evaluation is desired for the problem, this criterion might be used as a limitation for the maximum pressure. Keeping the loading below this limit induces an elastic behaviour for the structure and therefore ensures the complete re-establishment of the original geometry after the imposed loading is removed. Even in the case of more sophisticated inelastic analysis which surpasses this loading situation, keeping this parameter in mind brings intuition for the designer on how much he/she has advanced on areas of the design which contain larger uncertainty (for example material post-elastic behaviour, complete isotropy of steel after yielding, not-homogeneous distribution of plastic strains, etc.)

Hydrostatic pressure which would lead to the yielding of the hull`s plate center at the interframe midbay ($P_{center_yield_midbay}$)

In accordance to the failure condition proposed by Pulos [19] and studied by Reijmers [17], this parameter can be used to characterize the limiting pressure for the interframe hull plate. The results obtained numerically by Reijmers from full non-linear numerical analysis of typical geometries presented reasonable matching to existing analytical formulae for the interframe collapse.

The assumption for such failure mode consideration is that full plasticity occurs when the fibre at the center of the hull`s plate at mid-bay reaches the Von-Mises stress. In this condition, all plastic reserve would have been consumed and axisymmetric failure (accordion mode) occurs. The small plastic reserve existent at the hull`s plate at the frame`s location is ignored, and it is also assumed that the hoop stress are mainly compressive membrane stresses (negligible bending arises just from Poisson`s effect).

Hydrostatic pressure which would lead to the yielding of the outer fiber of a ring stiffener flange
(P_{flange_yield})

This failure mode is based on the hypothesis that usually ring stiffened structures have little plastic reserve when global failure modes are contemplated. The bending effects which arise at the ring frames from the unavoidable out-of-circularity are magnified by the important geometrical non-linear effects and the structure reaches an ULS when the yield stress is reached at the outer fiber of a ring stiffener flange.

So, this parameter can be considered as an important representation of possible global collapse of the stiffened compartment.

Hydrostatic pressure which is obtained at the last converged analysis step (P_{last_conv})

This failure mode is based on the premise that a static analysis is being performed and that the numerical analysis model can no longer reach force equilibrium at the stage when all plastic hinges are formed, and all plastic reserve is consumed.

Of course, this parameter is highly dependent on the settings for the non-linear numerical analysis settings like time stepping, solver type, convergence criterion, etc. but it is a very good indicative on the upper bound collapse capacity that can be reached numerically.

Hydrostatic pressure related to the Linear Buckling Eigenvalue of the first mode ($P_{lin_buckling}$)

The pressure obtained from the buckling eigenvalue analysis is not directly related to the global collapse, since it usually is associated with unrealistic failure modes which would arise from construction imperfections with a high number of interframe lobes around the circumference (e.g., for typical geometries the shape of the first eigenmode can have 15 interframe lobes around the circumference [17]), but it is the numerical value which provides the upper bound for the capacity obtained from a non-linear analysis. Also, methodologies exist to conservatively determine the collapse pressure by the use of the linear buckling eigenmodes, like the “Determination of buckling resistance by use of linearized buckling values” as described in [2].

So, this is a relevant parameter to be tracked in the present study.

4.8. Statistics and Uncertainty Quantification

The uncertainty quantification for each level of expertise is made using two different approaches (both bring different understandings for the uncertainty value), one makes use of the Estimated Coefficient of Variation and the other is made by means of the 95th quantile assuming the model results are samples from a population who is governed by a distribution with the same shape as of a Student’s t-distribution.

The assumption of the shape of a Student’s t-distribution for the population of results is made in order to make the probabilities more realistic for the cases where only a few samples were produced (e.g., for the only three models constructed under the assumption of an Expert User). In this case, the number of degrees of freedom is small and the Student’s t-distribution produces heavier tails to account for the larger possibilities of having values far from the mean. In the case of the results which could be produced by an Advanced beginner, thirty models were constructed (therefore the number of degrees of freedom is twenty-nine) and the Student’s t-distribution is very close to a normal gaussian distribution.

In the tables presented in chapter 5.5.1, as an additional indication on the possible variability of the data, the lower and upper bounds for a 95% confidence level for the mean values are shown (obtained from a t-distribution). Those values give an interpretation on how far the average values from the set can be from the true mean value, considering in this case that the population related to each result set is normally distributed.

Quantification by the Estimated Coefficient of Variation (U_{CV})

This is the ratio of the estimated standard deviation (the standard deviation of the captured responses when considered as samples from a larger population) to the mean value of the samples. It is a nice representation of the dispersion of the data and very useful to compare the variability of different data sets with different mean values.

Quantification by the 95th Quantile (U_{95})

This uncertainty quantification is defined here as the ratio between the 95th quantile of the data set to its estimated mean. It can be understood as a safety value that tells us that there is only a five percent probability that the obtained variation (in terms of a percentage to be applied over the estimated mean) will be exceeded. This is a value which can easily relate to current design codes.

The 95th quantile of the data can be obtained by multiplying the estimated standard deviation from each data set by the quantiles from standard tables for the t-distribution (for one-sided confidence interval) and adding this to the estimated mean value. In this research, the values of interest for the t-distribution quantiles are presented in Table 5 below (taken from [20]):

Table 5 – Student’s t-distribution one-sided quantiles of interest

| Level of Expertise | Quantity of samples | Degrees of Freedom | t-distribution 95 th Quantile |
|---------------------|---------------------|--------------------|--|
| Advanced Begginer | 30 | 29 | 1.699 |
| Competent Performer | 18 | 17 | 1.734 |
| Expert Performer | 3 | 2 | 2.920 |

Comparison between Levels of Expertise

The uncertainty attained for each level of expertise are then analysed together in order to derive a possible quantification on how much the results from an Advanced beginner can vary in relation to the ones obtained by an Expert performer. The approach for this comparison is made by assuming that the expert’s results would only slightly fluctuate around an average value and the Advanced Beginner’s results (with larger scatter) would be safely characterized by its 95th quantile. The ratio between both values mentioned above would bring an intuition on how much variation the results of an Advance Beginner would have in relation to the ones prepared by an Expert Performer.

5 Analysis and Discussion of the Results

5.1. Software

All models in this study were constructed using the Ansys Workbench 2019 R1 framework. All geometries were constructed in the DesignModeler 2019 R1 interface and the analysis performed in the Ansys Mechanical 2019 R1 software.

5.2. Non-linear Settings

The non-linear analysis was forcibly subdivided in two hundred time steps and at each step the corresponding fraction of the final load (1/200 of the total load of 10Mpa) was applied. This means that the auto-time-stepping capabilities of the program is turned off and that all models have the same load increment pattern. Other aspects which arise from this is that the resolution of the non-linear analysis and the results is of 0.05Mpa, related to a submergence of around 5 meters. The Linear Elastic Eigenvalue buckling analysis keeps its large resolution since it independent of this time stepping.

The Solver used is a Direct Solver (Sparse Ansys Solver is used) with the Large Deflection Option turned On or Off depending on the constructed model.

The default options for the convergence criteria and the Line search capability are used, and the Stabilization technique (addition of artificial dampers to improve convergence) is turned off.

The analysis is of a Load controlled type, where the time steps are controlled by load increments (as opposed to a displacement control type). And, since neither the Arc Length method, nor the Riks method are used, the post-instability behaviour cannot be captured.

The Buckling Eigenvalue analysis is run upon the pre-stressed configuration when 1.0 MPa is applied.

5.3. Model Quantities and Run Time

In general, the analysis took around 15 minutes for the very coarse meshes and 4 hours for the very fine meshes until the not converged load steps were reached.

Table 6 below brings the quantity of model entities for the smallest model and for the largest model.

Table 6 – Model Quantities

| | Mesh Size | Element Order | Number of Nodes | Number of Elements |
|----------------|-----------|---------------|-----------------|--------------------|
| Smallest Model | 0.26m | Linear | 1334 | 1267 |
| Largest Model | 0.0325m | Quadratic | 153677 | 50958 |

5.4. Mesh Convergence Studies

The mesh convergence study for some key responses are demonstrated in Figure 18 and Figure 19. The first plot gives an indication that the model has converged for the smallest three mesh sizes in terms of a global elastic behaviour. It is interesting to note how the models with the quadratic elements (models 1 and 4) approach convergence faster. Also, it can be noticed that the large displacements option does not have major influence in the Linear Elastic Buckling Pressure (e.g., Models 2 and 5 follow approximately the same line). This is expected since the Linear Elastic Buckling pressure is in general independent on how the non-linear geometrical aspects are defined.

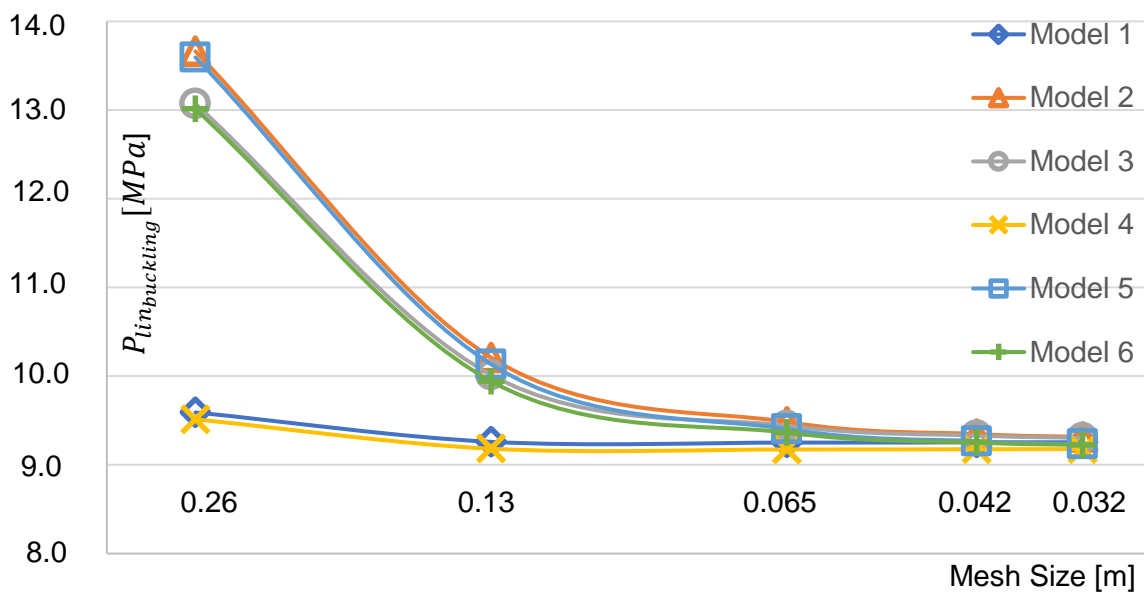


Figure 18 – Mesh Convergence study for the Eigenvalue Buckling Pressure – Log Scale

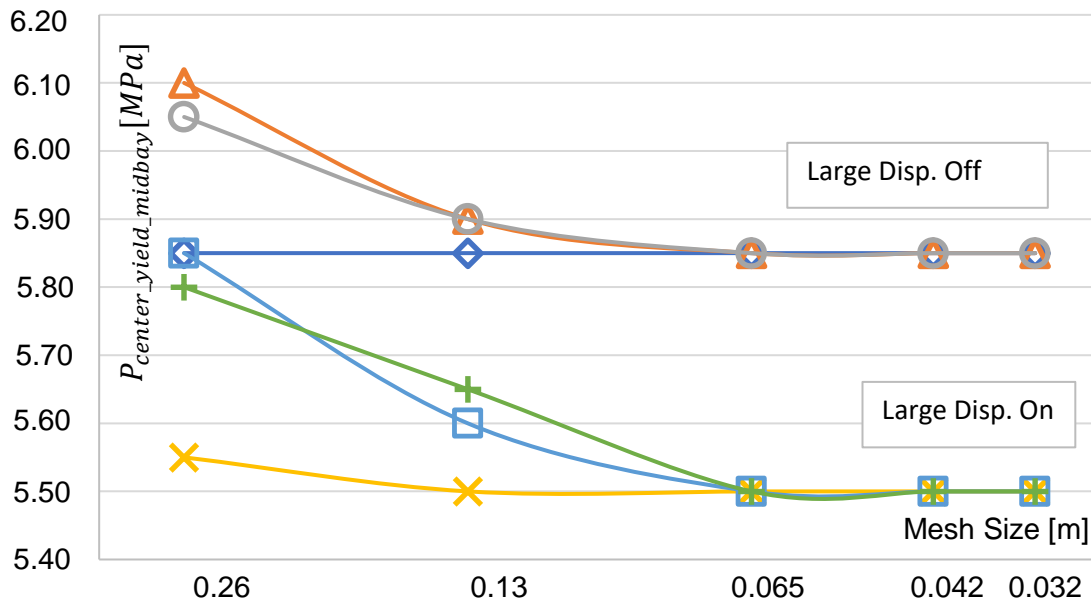


Figure 19 - Mesh Convergence study for the pressure which induces yielding of the hull's plate center at the interframe midbay– Log Scale

The parameter to track in the second plot was selected as the indication for stress convergence since at midbay no singularities are present (i.e., both at stiffener and at flange location singularities would affect the convergence results). Again, quadratic elements approach convergence much faster, but towards two different plateaus, dependent on how each model is set for Large Displacements. This is also expected since, when the large displacements are on, the updating of the stiffness matrix at each time step induces a softening of the structure which increases the geometrical non-linear effects and the yield at the tracked location is reached faster.

5.5. Results and Their Uncertainty Quantification

5.5.1. Uncertainty Quantification Within Each Level of Expertise Group

Each subsection below starts by presenting a table with the statistical summary of the possible results obtained by analysts at each expertise level. The related data is then presented in plots separated for each tracked failure related response.

In Table 7 to Table 9, ST_DEV is the estimated Standard Deviation; 95_quantile is the ninety fifth quantile. LB_AVR95 and UB_AVR95 are the lower and upper bounds for the average with a 95% confidence level, respectively. U_{95} U_{CV} are defined in chapter 4.8.

Expected Uncertainty in Results Obtained by Advanced Beginners Analysts

The values from Table 7 demonstrates that a variability of 3.34 % to 3.61% can be expected in terms of the estimated Coefficient of Variation (U_{CV}) for the yield pressures obtained in non-linear analysis which could be performed by an Advanced Beginner. The value for the last convergence displays a larger scatter ($U_{CV} = 6.06\%$), but the largest variability for this level of expertise would be present when capturing the $P_{lin_buckling}$ ($U_{CV} = 13.92\%$).

Table 7 - Expected Uncertainty in Results obtained by Advanced Beginners Analysts

| Response | Average [MPa] | UB_AVR95 [MPa] | LB_AVR95 [MPa] | ST_DEV [MPa] | 95_quantile [MPa] | U_{95} [-] | U_{CV} [-] |
|-----------------------------|---------------|----------------|----------------|--------------|-------------------|--------------|--------------|
| P_{1st_yield} | 5.05 | 5.11 | 4.98 | 0.18 | 5.36 | 6.14% | 3.61% |
| P_{flange_yield} | 5.19 | 5.25 | 5.12 | 0.19 | 5.50 | 6.10% | 3.59% |
| $P_{center_yield_midbay}$ | 5.73 | 5.80 | 5.65 | 0.19 | 6.05 | 5.67% | 3.34% |
| P_{last_conv} | 6.06 | 6.20 | 5.92 | 0.37 | 6.68 | 10.30% | 6.06% |
| $P_{lin_buckling}$ | 9.95 | 10.46 | 9.43 | 1.38 | 12.30 | 23.65% | 13.92% |

The plots shown in Figure 20; Figure 21 and Figure 22 presents a clear separation between the results from the models with or without the Large Displacements consideration. This is due to the structural softening which arises from the geometrical non-linearities already mentioned previously in this document. That is not the case for the plot at Figure 23, since it plots results for Linear Buckling Analysis, for which the non-linear geometrical settings do not play a major role.

Figure 20 demonstrates that results with a very coarse mesh, linear elements and large displacements off (Model types 2,3) tends to largely overestimate $P_{center_yield_midbay}$, but the quadratic elements with large displacements on (related to model type 4) apparently produce sufficiently good results for this response even when a very coarse mesh is used.

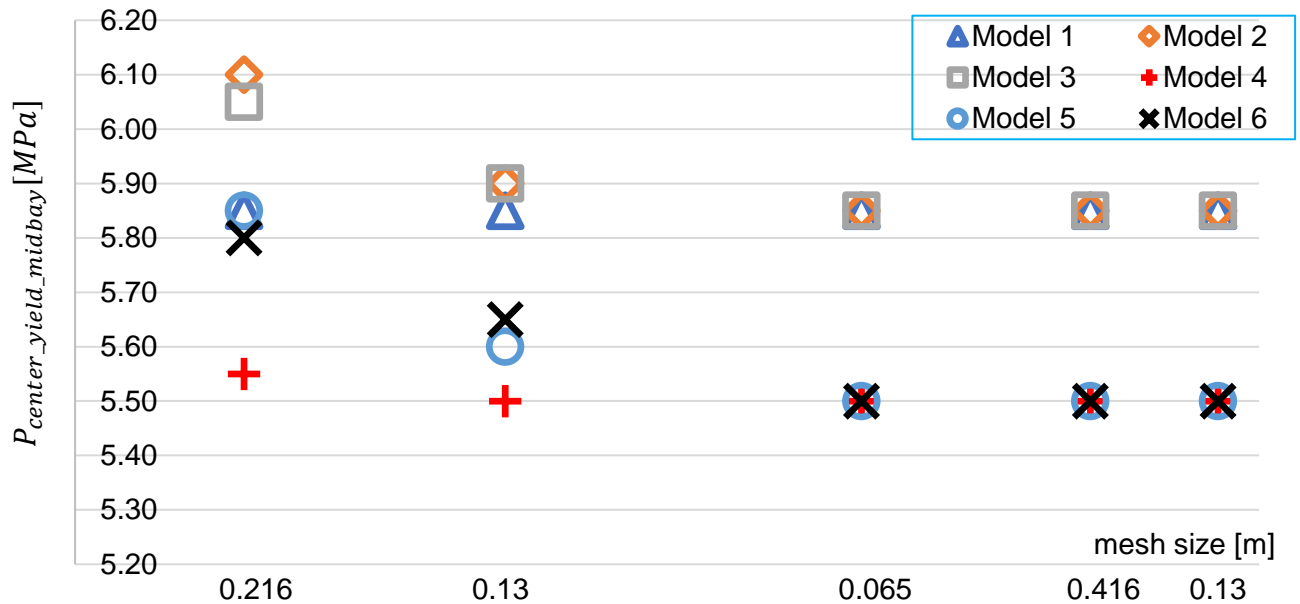


Figure 20 - Possible Results by Advanced Beginners - $P_{center_yield_midbay}$

It can be seen when comparing the results from Model 2 (linear elements with reduced integration) to Model 3 (linear elements with full integration) in Figure 21 that the in plane integration scheme plays a role in how the convergence is approached in very fine meshes.

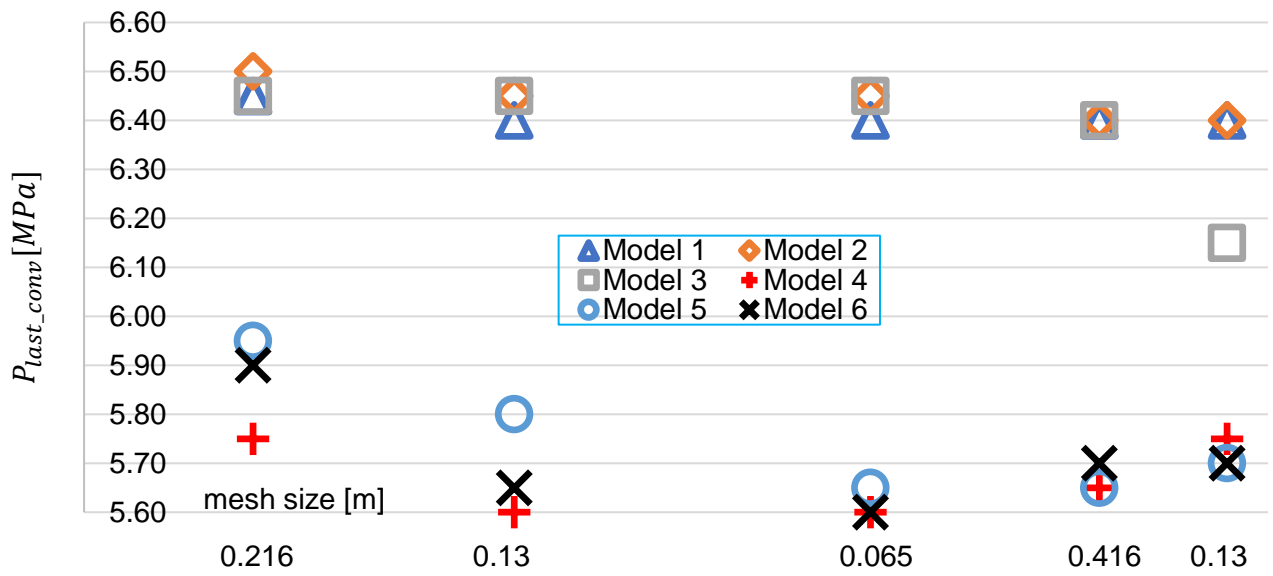


Figure 21 - Possible Results by Advanced Beginners - P_{last_conv}

One interesting aspect of the plot in Figure 22 is to notice that models with quadratic elements (Models 1 and 4) present a larger scatter when P_{1st_yield} is tracked. The reasoning behind this might be the fact that quadratic elements can be more susceptible to steep stress increases which arise due to singularities (i.e., from the higher order interpolation function used), and therefore the mesh variation has larger impact on the value of pressure for which yield would be reached in the model.

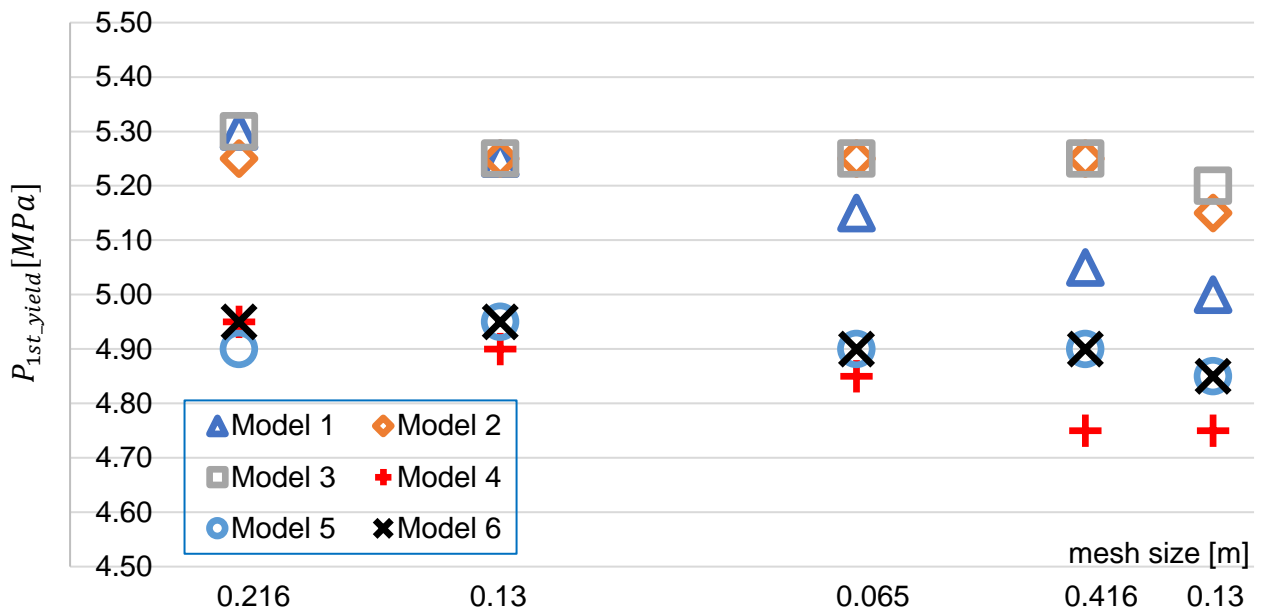


Figure 22 - Possible Results by Advanced Beginners - P_{1st_yield}

Figure 23 presents the fact that, in the same manner as in Figure 20, very coarse meshes used with linear elements (Model types 2,5, 5 and 6) might greatly overpredict buckling results.

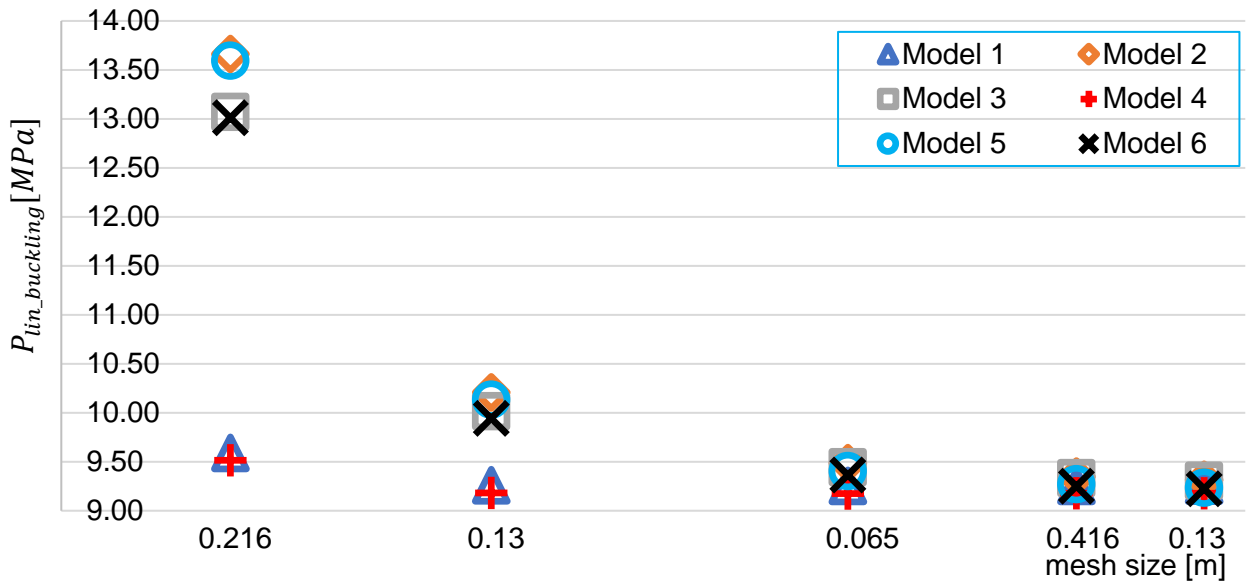


Figure 23 - Possible Results by Advanced Beginners - $P_{lim_buckling}$

And Figure 24 demonstrates that the pressure which leads the yield at the flange to be reached, might be under estimated if using very coarse meshes and linear elements (Model types 2,3,5 and 6 present smaller pressures for very coarse mesh than the converged values). Probably this fact arises from the very poor discretization condition along the stiffener's flange.

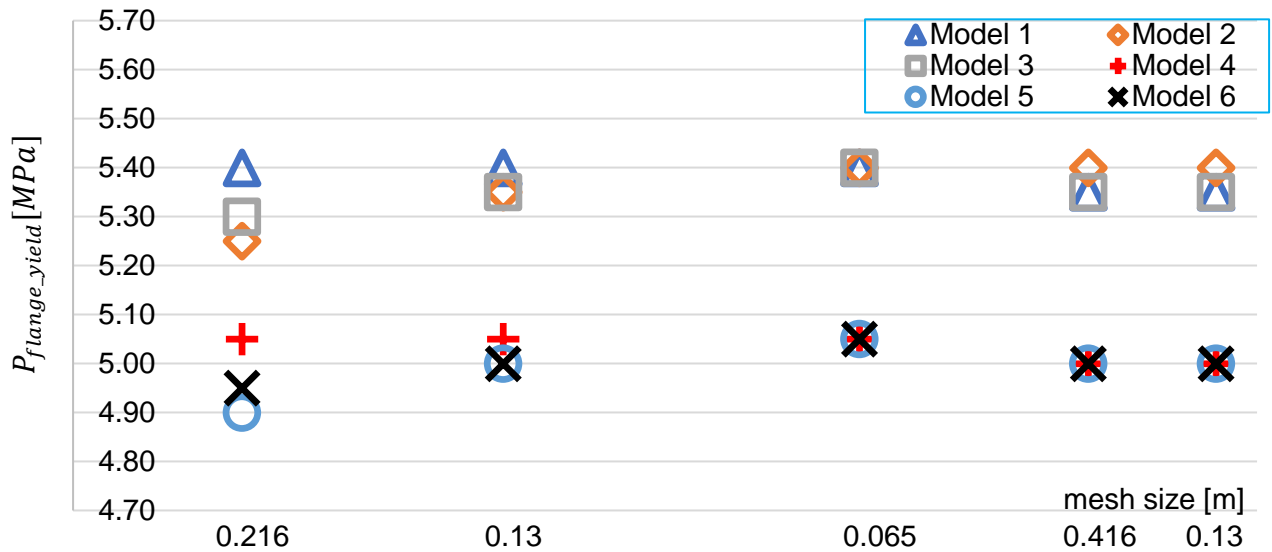


Figure 24 - Possible Results by Advanced Beginners - P_{flange_yield}

Expected Uncertainty in Results Obtained by Competent Performers Analysts

While analysing Table 8 it can be perceived that the variability in terms of U_{CV} for the yield pressures obtained in non-linear analysis by Competent Performers have approximately the same magnitude than the ones obtained by Advanced beginners (they range from 3.17% to 3.65%). This is from the fact that the major source of variability (i.e., the consideration or not of large displacements) is still present. A major difference from the results which could be obtained by Advanced Beginners is present in the U_{CV} for the $P_{lin_buckling}$, which is now greatly reduced. The reason for this is the assumption that a Competent Performer would filter out from its analysis the results obtained from grossly wrong meshes.

Table 8 - Expected Uncertainty in Results obtained by Competent Performers Analysts

| Response | Average [MPa] | UB_AVR95 [MPa] | LB_AVR95 [MPa] | ST_DEV [MPa] | 95_quantile [MPa] | U_{95} [-] | U_{CV} [-] |
|-----------------------------|---------------|----------------|----------------|--------------|-------------------|--------------|--------------|
| P_{1st_yield} | 5.01 | 5.10 | 4.92 | 0.18 | 5.33 | 6.35% | 3.65% |
| P_{flange_yield} | 5.20 | 5.29 | 5.10 | 0.19 | 5.52 | 6.28% | 3.61% |
| $P_{center_yield_midbay}$ | 5.68 | 5.76 | 5.59 | 0.18 | 5.99 | 5.52% | 3.17% |
| P_{last_conv} | 6.03 | 6.21 | 5.84 | 0.38 | 6.68 | 10.84% | 6.23% |
| $P_{lin_buckling}$ | 9.29 | 9.34 | 9.25 | 0.09 | 9.45 | 1.68% | 0.97% |

The plots presented in Figure 25 to Figure 29 demonstrate clearly the role of the large displacements in the variability (difference between model types 1,2,3 and 4,5,6). The tracked response which is significantly impacted by meshing when only the model types from competent users are considered is the P_{1st_yield} presented in Figure 27. This effect might again be related to the effect that singularities have upon stresses results at the flanges and at the stiffeners (singularities exist due to the interface to the web elements).

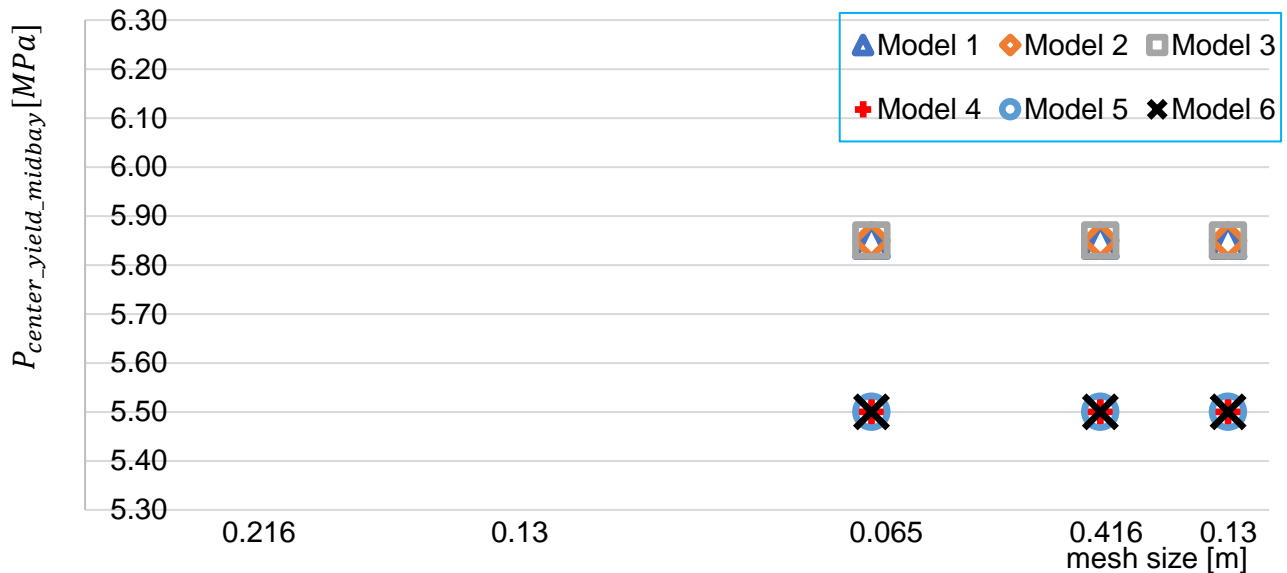


Figure 25 - Possible Results by Competent Performers - $P_{center_yield_midbay}$

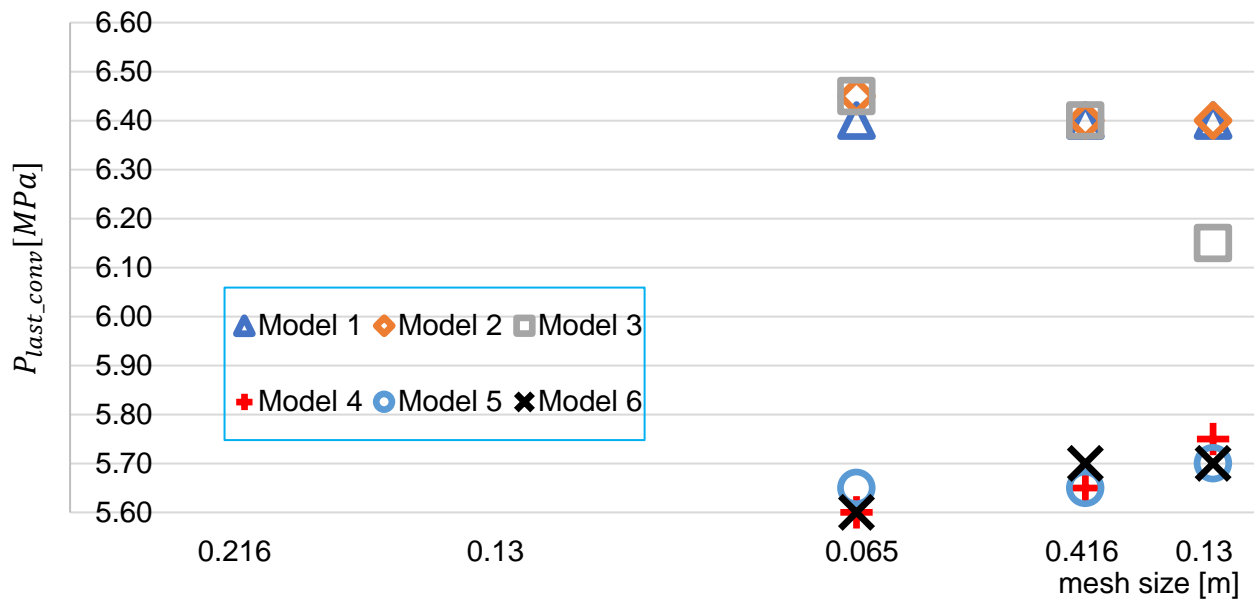


Figure 26 - Possible Results by Competent Performers - P_{last_conv}

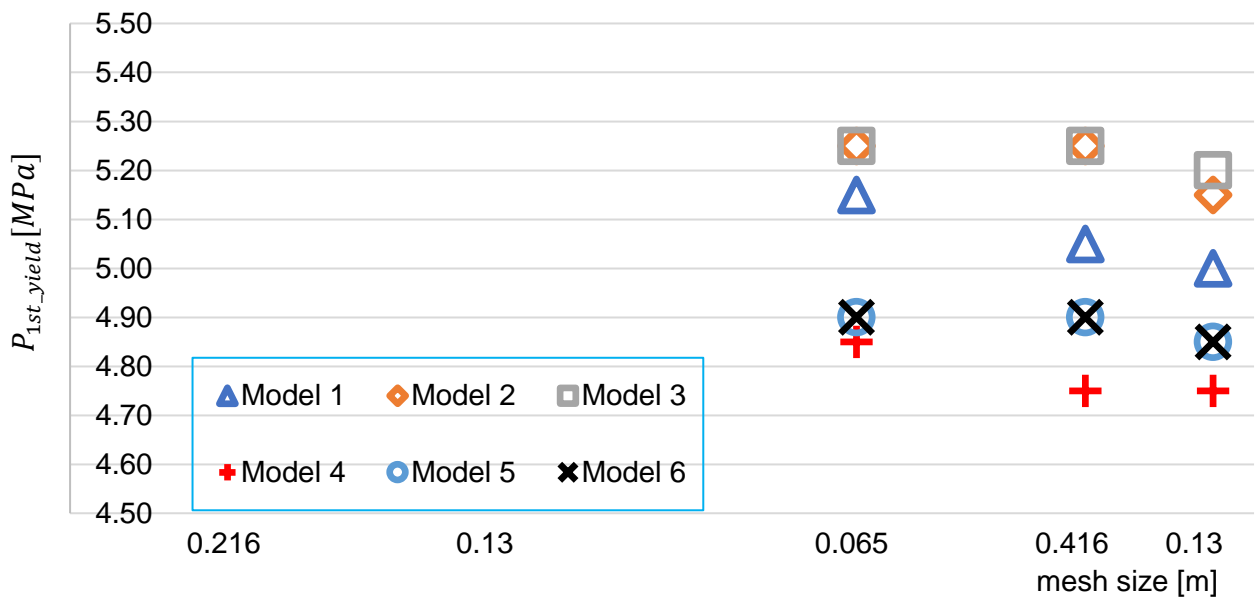


Figure 27 - Possible Results by Competent Performers - P_{1st_yield}

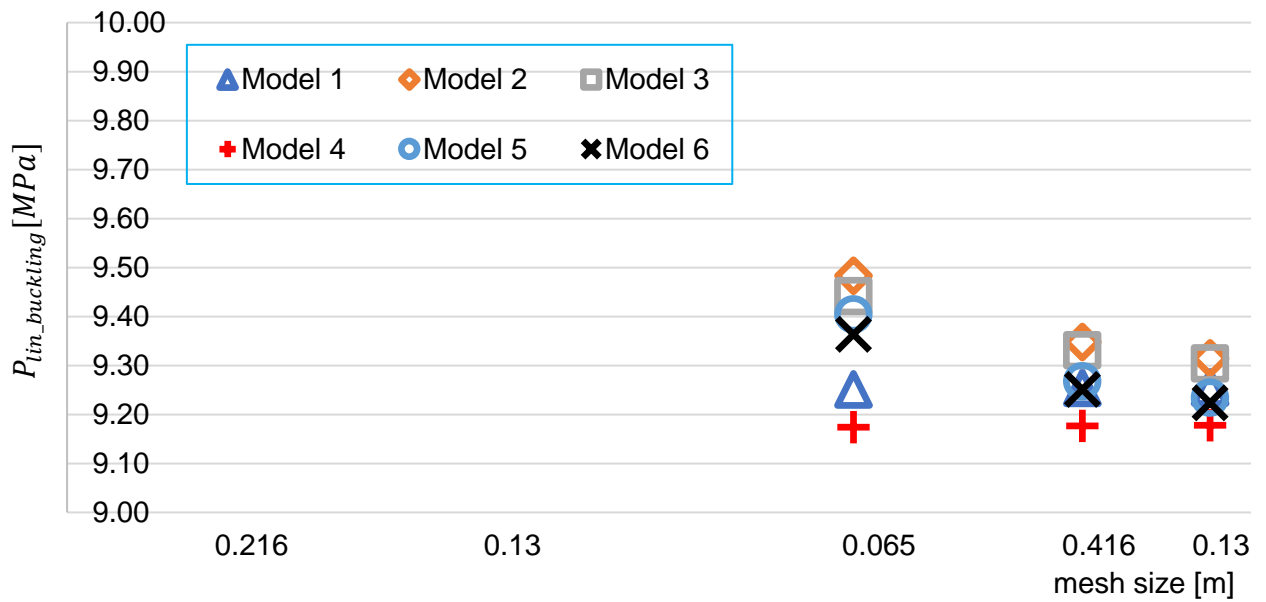


Figure 28 - Possible Results by Competent Performers - $P_{lin_buckling}$

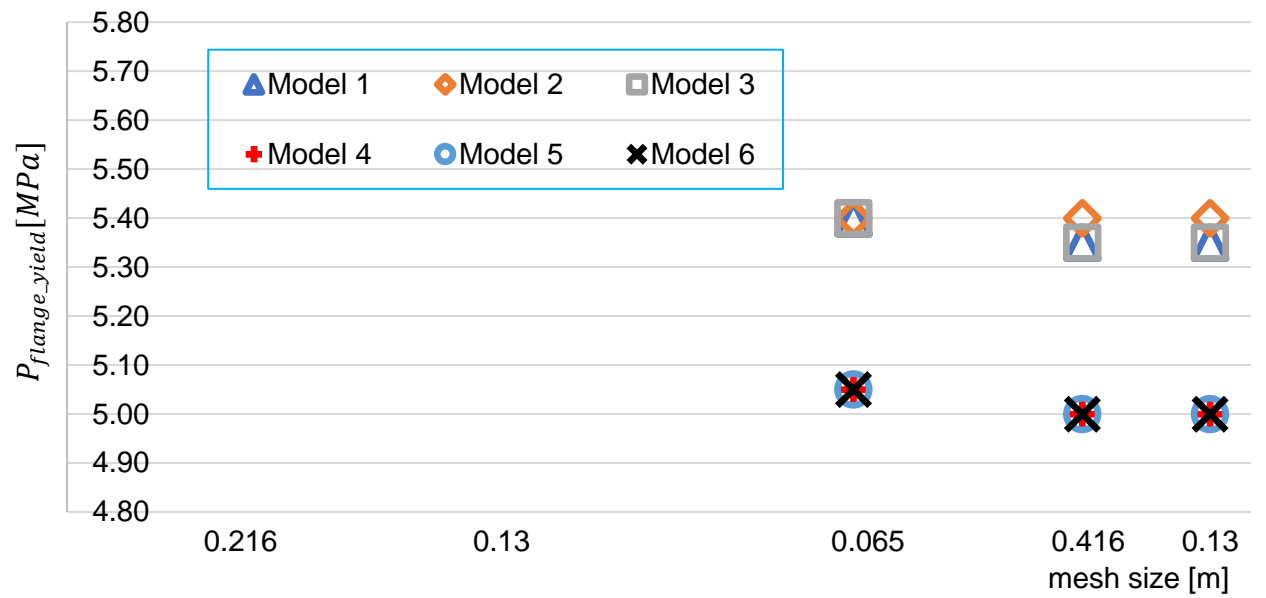


Figure 29 - Possible Results by Competent Performers - P_{flange_yield}

Expected Uncertainty in Results Obtained by Expert Performers Analysts

The results shown at Table 9 clearly show that the expected variability in the results obtained by an Expert Performer Analyst would be very small, both in terms of U_{95} and U_{CV} . This is due to the fact that only meshes with proper converged responses and the correct physics assumption (Large Displacements turned on) are used. It is important to note that, in general, the average values presented in Table 9 are smaller than the ones presented in tables Table 7 and Table 8, meaning that both Advanced Beginners and Competent Performers might produce over predicted results for collapse pressures.

Table 9 - Expected Uncertainty in Results obtained by Expert Performers Analysts

| Response | Average [MPa] | UB_AVR95 [MPa] | LB_AVR95 [MPa] | ST_DEV [MPa] | 95_quantile [MPa] | U_{95} [-] | U_{CV} [-] |
|-----------------------------|---------------|----------------|----------------|--------------|-------------------|--------------|--------------|
| P_{1st_yield} | 4.78 | 4.93 | 4.64 | 0.06 | 4.95 | 3.52% | 1.21% |
| P_{flange_yield} | 5.02 | 5.09 | 4.94 | 0.03 | 5.10 | 1.68% | 0.58% |
| $P_{center_yield_midbay}$ | 5.50 | 5.50 | 5.50 | 0.00 | 5.50 | 0.00% | 0.00% |
| P_{last_conv} | 5.67 | 5.86 | 5.48 | 0.08 | 5.89 | 3.94% | 1.35% |
| $P_{lin_buckling}$ | 9.18 | 9.18 | 9.17 | 0.00 | 9.18 | 0.07% | 0.02% |

Figure 30 shows that for the region far from singularities (at midbay) models with quadratic elements have presented complete convergence already with reasonably sized meshes

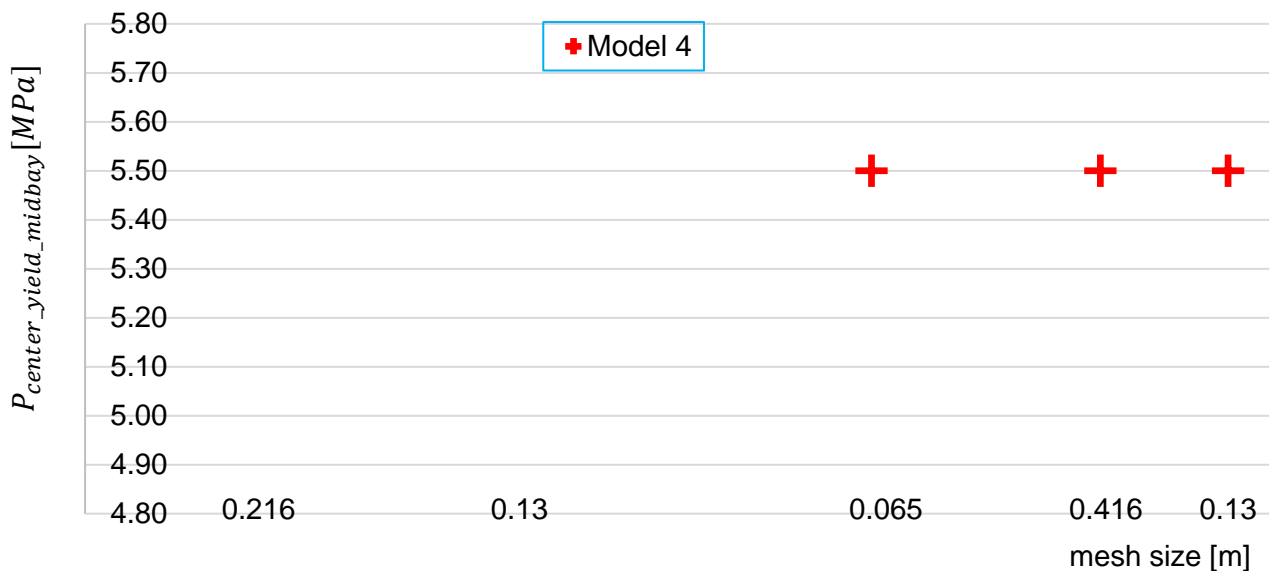


Figure 30 - Possible Results by Expert Performers - $P_{center_yield_midbay}$

Now Figure 31, brings light on the condition that the quadratic elements used by the Expert Performer would predict a slightly smaller P_{last_conv} when reasonably sized meshes are used for the problem (0.065m). This demonstrates that the finer the mesh, the greater the ability for the numerical solver to reach a stable solution.

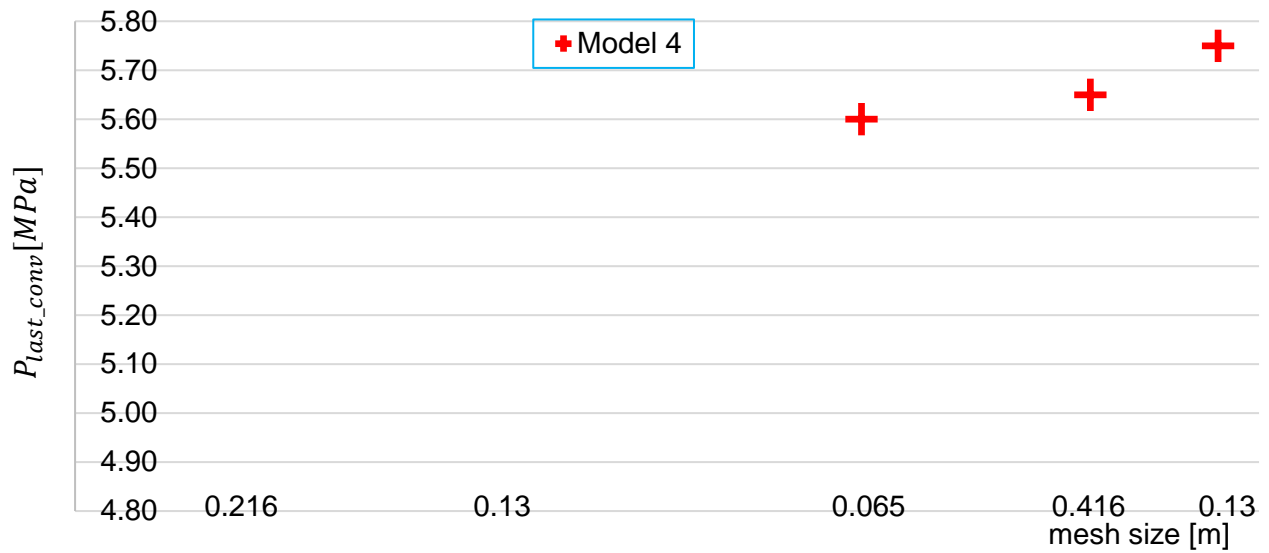


Figure 31 - Possible Results by Expert Performers - P_{last_conv}

Figure 32 demonstrates that the very fine meshes bring slightly smaller P_{1st_yield} . Since first yield for expert users is at the stiffener location, this might again be explained by the singularity present between the stiffener web and the hull plate.

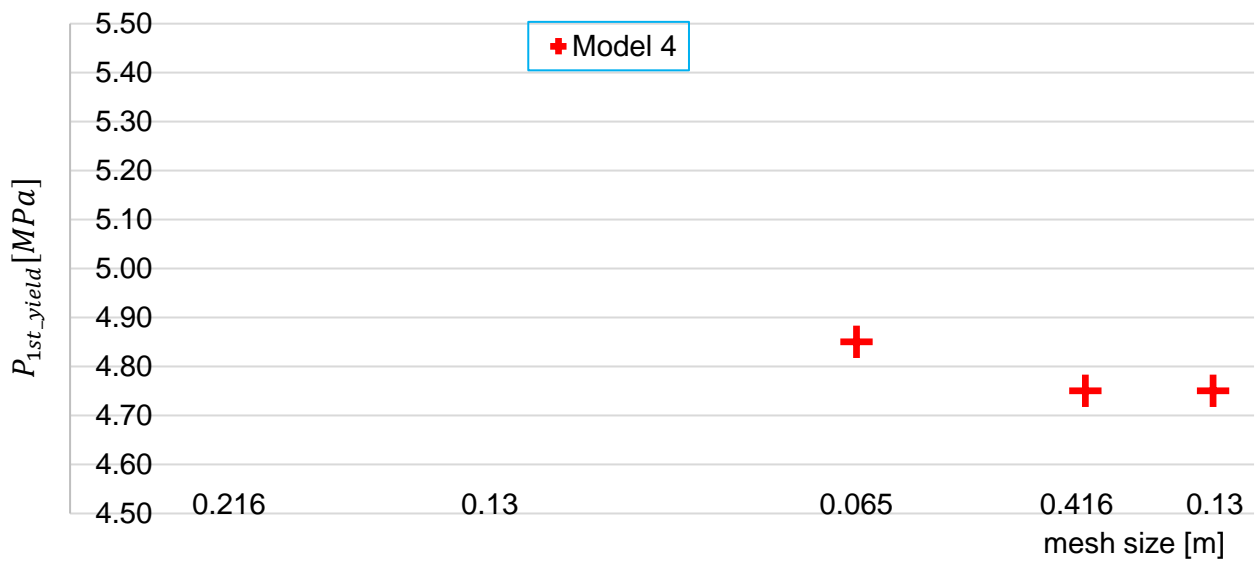


Figure 32 - Possible Results by Expert Performers - P_{1st_yield}

It can be perceived in Figure 33 that for $P_{lin_buckling}$ all three mesh sizes considered in an Expert Performer analysis would have already presented complete convergence.

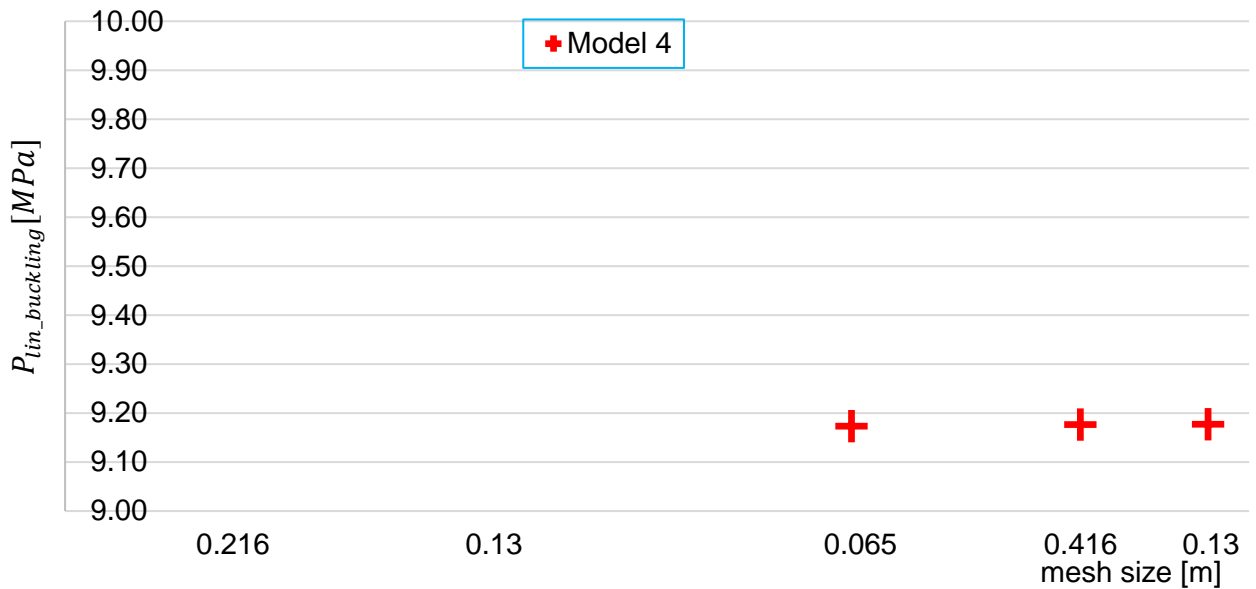


Figure 33 - Possible Results by Expert Performers - $P_{tin_buckling}$

Finally, Figure 34 illustrates the fact that when quadratic elements are considered, the reasonably sized meshes (i.e., with element size of 0.065m) would produce slightly higher predictions for P_{flange_yield} .

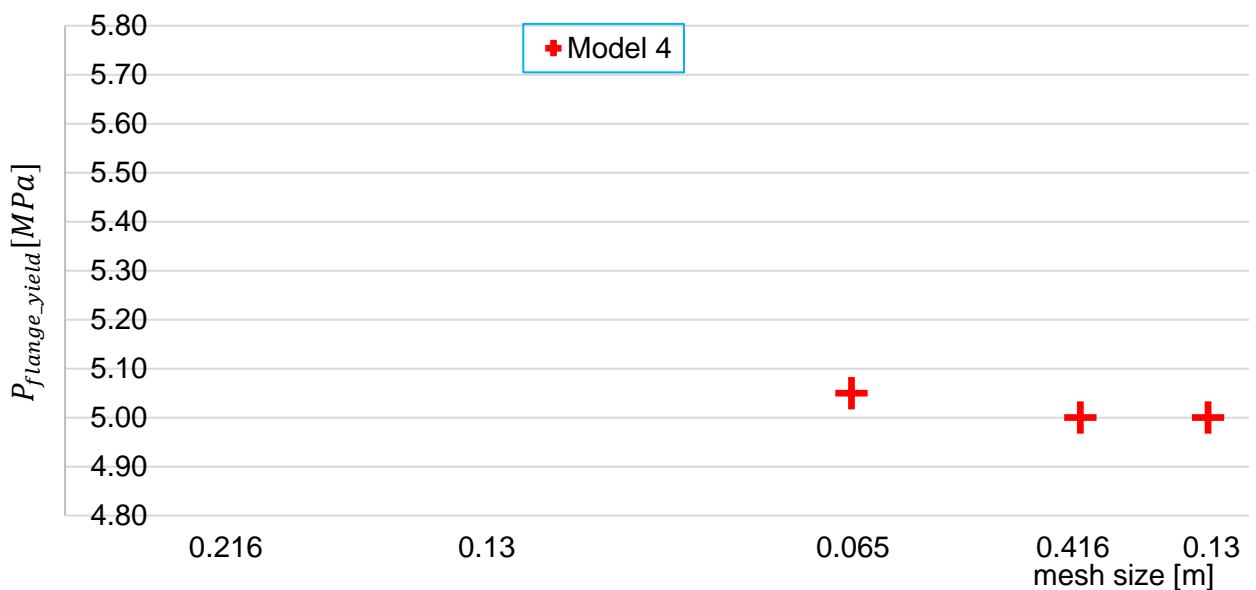


Figure 34 - Possible Results by Expert Performers - P_{flange_yield}

5.5.2. Uncertainty Quantification Between Different Levels of Expertise

Confirming the reasoning made on chapter 4.8, the results from an Expert Performer would have a much smaller scatter than the ones predicted by an Advanced Beginner (see chapter above). In this sense, it is assumed here that the results from an Expert Performer might be characterized by its average, but in order to be certain on a value not to be exceeded, the results from an Advanced Beginner would be characterized by its 95th quantile.

The ratio between both values above gives an indication on how much one can expect as variability from a finite element model result in problems similar to the one studied here when no information is given about the level of expertise of the analyst.

Table 10 below provides the above-mentioned ratio for all tracked responses. A variability of 9.66 % to 11.98% can be expected for the pressures which lead to yield at key locations obtained in non-linear analysis. A much larger value could occur for the $P_{lin_buckling}$ and the cause for this is that this parameter is highly dependent on the possible meshes variation for the Advanced beginner analysis.

Table 10 - Ratio 95th quantile [adv_begginer] / Average [expert performer]

| Failure Pressure | Ratio 95 _{quantile} [adv_begginer] / Average [expert] |
|-----------------------------|--|
| P_{1st_yield} | 11.98% |
| P_{flange_yield} | 9.66% |
| $P_{center_yield_midbay}$ | 9.99% |
| P_{last_conv} | 17.96% |
| $P_{lin_buckling}$ | 34.05% |

As an additional clarification, Figure 35 visually displays both probability distributions (considering the shape of a Student's t- distribution) for the Advanced Beginner and the Expert Performer for the P_{flange_yield} . The distributions are obtained from the estimated average and standard deviation presented in Table 7 and Table 9 and the degrees of freedom obtained as the quantity of models from Table 3 minus one. The distance which is related to the ratio in Table 10 is also shown.

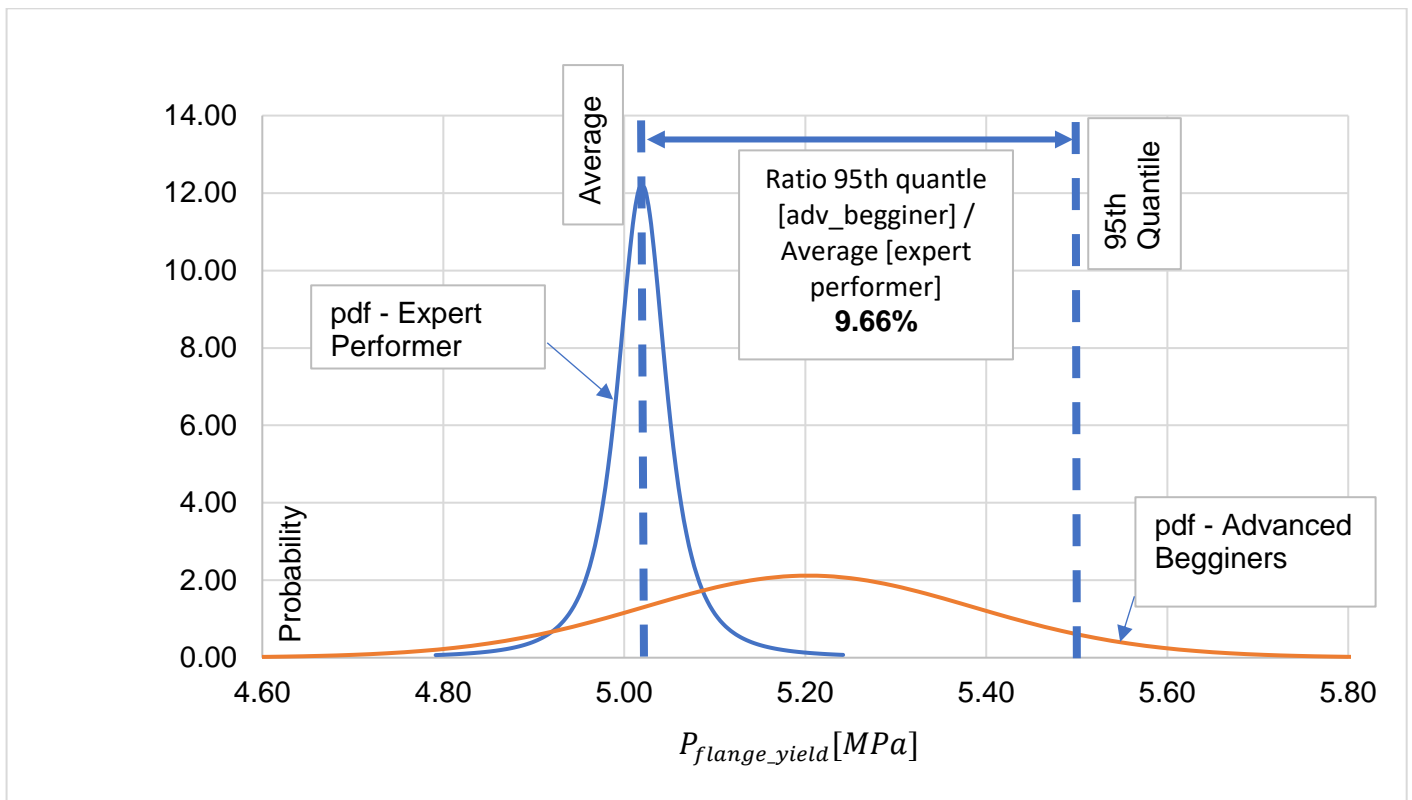


Figure 35 - Uncertainty Comparison between different levels of expertise for P_{flange_yield}

On Figure 35, the thicker tails expected from the shape of the Student's t-distribution can be noticed on the pdf for the Expert Performer. This arises from the small quantity of samples related to possible models from Expert Performers in this research. The tails of the Advanced Beginner's pdf resemble the tail from a Gaussian distribution, since the quantity of degrees of freedom is large (close to 30).

6 Conclusions

As a general understanding from the study performed, it could be perceived by the author that the uncertainty in finite element modelling is deeply related to the level of expertise of the analyst. A relevant scatter was perceived when capturing possible results from Advanced Beginners (see Table 7). But, if the model is prepared by an Expert Performer using the correct physics and the proper methodologies for the meshing and the parameter's setting, the uncertainty in the results are expected to be small (see Table 9).

On the other hand, it seems easy that in industry practice important details on the analysis setting can go unnoticed even by Competent Performers and the results can be significantly impacted by this. An important example of this is the consideration of the large displacements during the analysis. With small displacements values at hand, many analysts might judge the displacements to be small enough to be negligible and set the large displacements option to be off, in order to expedite the analysis. But, as demonstrated in Table 10, this can lead to important problematic over prediction of collapse pressures.

From the parameters studied for the problem presented in this thesis, two stood out as major sources of uncertainty, (1) the mesh size and (2) the large displacements consideration. The first is related to solution approximation errors and is a manifestation of the differences between numerically solving the equation and the exact analytical solution. The second is related to model form errors which arises from the incapacity of the selected model to completely represent the real phenomenon.

Other model form errors like boundary conditions or material aspects were not explored in this thesis, since it was assumed that analysts within all levels of expertise would be able to filter out the grossly incorrect physical assumptions. But anyway, during the exercise of preparing the models for this thesis, when for example small errors in setting symmetry conditions were made, it was perceived by the author that for sure they would bring large impact on the obtained results.

Other parallel conclusion which could be drawn from the study, not necessarily related to uncertainty but which is interesting to report, is the fact that the results from Expert Performers for this problem presented $P_{center_yield_midbay}$ with a collapse pressure much closer to P_{last_conv} than the P_{flange_yield} (see the average values in Table 9). This means that, although yield has been reached at the stiffener's flange, the structure still had relevant reserve before its collapse (which was governed by the yield at midbay). This result obtained numerically contradicts the analytical assumptions for global collapse which considers that, with little plastic reserve, overall collapse is reached when the yield stress in the outer fibre of the flange of the ring frame is reached. So, there is a chance that the analytical formulation might be predicting global collapse with conservativeness in excess. This can be perceived by analysing Table 9, where the average for P_{last_conv} is 12.94% higher than P_{flange_yield} .

The author's hypothesis for the contradiction above is the fact that the yield at the flange happens first where the out of circularity has its peak outwards (the stiffener region near the inward peak is still elastic). So, even after the first flange yielding, the stiffener's region near the inward peak might present sufficient stiffness by means of its bending to support some load redistribution from the yielded region of the flange. But this hypothesis is still to be confirmed by further studies.

Other suggestion for future studies which can arise from this research is to use this same problem as background to capture data from real life analysts with different levels of expertise, leaving the key parameters from this study open for their selection. This would allow the verification that the statistical assumptions made for the quantification of uncertainty in this study indeed hold.

Also, other possibilities for future research can be the use of the same analysis framework of this research applied to different problems (e.g., for different submarine classes, or with different magnitudes for the out-of-circularity). This could bring light on the problem dependency character of the obtained uncertainty. Future studies could also explore other solution approximation errors like the solver type (direct or iterative), out of plane integration scheme and the use or not of line search during the solving process.

Bibliography

- [1] Ultimate Strength Committee III, “5 - Benchmark Studies,” *19th International Ship and Offshore Structures Congress - ISSC*, vol. 1, pp. 322-336, 2015.
- [2] DNV GL, *DNVGL-RP-C208 - Determination of structural capacity by non-linear finite element analysis methods*, Høvik: DNV GL, 2016.
- [3] P. J. Frey and P.-L. George, *Mesh Generation Application to Finite Elements*, Second ed., London: ISTE Ltd and John Wiley and Sons, Inc, 2008.
- [4] Ultimate Strength Committee III, “9 - Benchmark Studies,” *20th International Ship and Offshore Structures Congress - ISSC*, vol. 1, pp. 394-424, 2018.
- [5] K.-J. Bathe, *Finite Element Procedures*, Second ed., Watertown, MA: K.J. Bathe, 2019.
- [6] B. Liang and S. Mahadeva, “Error And Uncertainty Quantification And Sensitivity Analysis In Mechanics Computational Models,” *International Journal for Uncertainty Quantification*, vol. 1, p. 147–161, 2011.
- [7] R. Rebba, *Model validation and design under uncertainty*, PhD thesis, Nashville, Tennessee: Vanderbilt University, 2005.
- [8] J. T. Oden, I. Babuska, F. Nobile, Y. Feng and R. Tempone, “Theory and methodology for estimation and control of errors due to modeling, approximation, and uncertainty,” *Computer Methods in Applied Mechanics and Engineering*, vol. 2, p. 195–204, 2005.
- [9] ANSYS, “ANSYS Mechanical User's Guide,” [Online]. Available: https://ansyshelp.ansys.com/account/secured?returnurl=/Views/Secured/corp/v193/wb_sim/ds_Home.html. [Accessed 03 December 2019].
- [10] E. N. Dvorkin and K.-J. Bathe, “A Continuum Mechanics Based Four-Node Shell Element For General Non-Linear Analysis,” *Eng. Comput*, pp. 77-88, March 1984.
- [11] X. Chen and Y. Liu, *Finite Element Modeling and Simulation with Ansys Workbench*, Boca Raton, FL: CRC Press, 2015.
- [12] J. Stoer and R. Bulirsch, *Introduction to Numerical Analysis*, Berlin Heidelberg: Springer-Verlag, 2002.
- [13] T. J. R. Hughes, *The Finite Element Method: Linear Static and Dynamic Finite*, Dover: Prentice-Hall, Inc, 2000.
- [14] E. Madenci and I. Guven, *The Finite Element Method and Applications in Engineering Using ANSYS*, New York: Springer, 2015.
- [15] J. T. Hackos and J. C. Redish, *User and Task Analysis for Interface Design*, New York, NY: John Wiley & Sons, Inc., 1998.
- [16] J. Reijmers, *Lecture Notes MT44035 - Structural design aspects of Submarine pressure hulls*, Delft: TuDelft, 2018.
- [17] J. Reijmers and D. Stapersma, “Uncertainty quantification with respect to global collapse of submarine pressure hulls compared to interframe collapse,” Nafems, Stockholm, 2017.
- [18] DNV GL, *NVGL-RU-NAVAL-Pt4Ch1 - Rules for classification, Naval vessels, Part 4 Subsurface*, Høvik: DNV GL, 2018.
- [19] J. G. Pulos, “Structural analysis and design considerations for cylindrical pressure hulls: DTMB report 1639,” Dept. of the Navy, David Taylor Model Basin, Washington, D.C., 1963.
- [20] R. V. Hogg, J. W. McKean and A. T. Craig, *Introduction to Mathematical Statistics (Eighth Edition)*, Boston, MA: Pearson, 2019.